GR2005-1

GEOSCIENTIFIC REPORT

Structure and geometry of the Paleoproterozoic Ruttan VMS deposit, southwest Rusty Lake belt (NTS 64B5), Manitoba

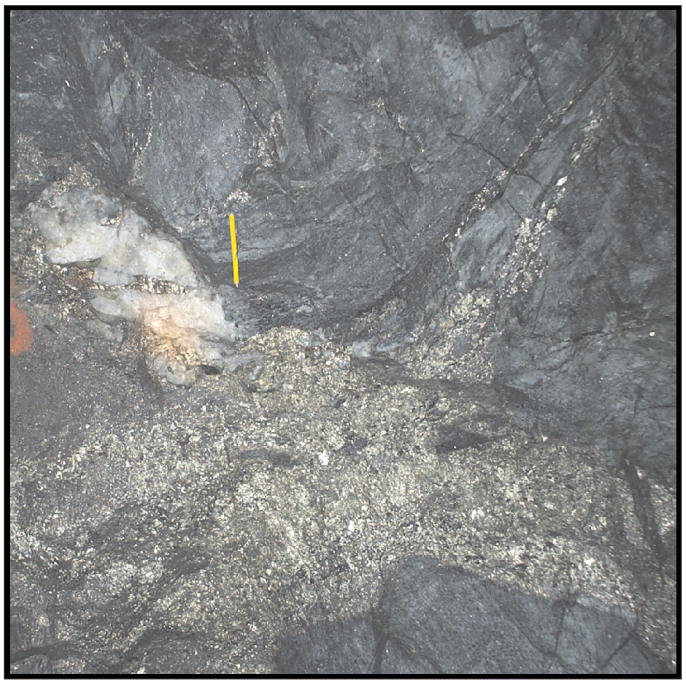

By
S.D. Anderson,
C.J. Beaumont-Smith
and C.O. Böhm

Manitoba

Geoscientific Report GR2005-1

Structure and geometry of the Paleoproterozoic Ruttan VMS deposit, southwest Rusty Lake belt (NTS 64B5), Manitoba

by S.D. Anderson, C.J. Beaumont-Smith and C.O. Böhm

Winnipeg, 2005

Industry, Economic Development and Mines

Hon. Jim Rondeau
Minister

Hugh Eliasson
Deputy Minister

Mineral Resources Division

C.A. Kaszycki
Assistant Deputy Minister

Manitoba Geological Survey

E.C. Syme
Director

Manitoba

Anderson, S.D., Beaumont-Smith, C.J. and Böhm, C.O. 2005: Structure and geometry of the Paleoproterozoic Ruttan VMS deposit, southwest Rusty Lake belt (NTS 64B5), Manitoba; Manitoba Industry, Economic Development and Mines, Manitoba Geological Survey, Geoscientific Report GR2005-1, 35 p.

NTS grid: 64B5

Keywords: Manitoba; Trans-Hudson Orogeny; Rusty Lake belt; Paleoproterozoic; Ruttan deposit; massive sulphide deposits; structural analysis; geometry; deformation; mineral deposits, genesis; tectonics, mineral exploration

Published by:
Manitoba Industry, Economic Development and Mines
Manitoba Geological Survey
360–1395 Ellice Avenue
Winnipeg, Manitoba
R3G 3P2 Canada
Telephone: (800) 223-5215 (General Enquiry)
(204) 945-4154 (Publication Sales)
Fax: (204) 945-8427
E-mail: minesinfo@gov.mb.ca
Website: http://www.gov.mb.ca/iedm/mrd/

Cover illustration: Irregular veins of strongly recrystallized, inclusion-rich solid sulphide (pyrrhotite-pyrite-chalcopyrite-sphalerite) cutting foliated volcaniclastic rocks in the footwall of the B lens, West mine (280mL level, 9B2 stope), Ruttan deposit. Late-tectonic emplacement of solid remobilized sulphide is indicated by the discordant, relatively undeformed aspect of the veins, and the presence of vein-quartz inclusions.

Abstract

The Ruttan volcanogenic massive sulphide (VMS) deposit is situated in the west-central portion of the Rusty Lake belt on the northern flank of the Paleoproterozoic Trans-Hudson Orogen in Manitoba. The deposit is hosted by ca. 1.91–1.88 Ga felsic metavolcanic rocks of the Mine Sequence unit (MSU), which are tectonically juxtaposed to the north and south, respectively, with ocean-floor mafic metavolcanic rocks of the Mill Pond unit and epiclastic metasedimentary rocks of the Powder Magazine unit. Overprinting relationships exhibited by mesoscopic deformation structures in the MSU indicate four phases of ductile deformation. The D_1 deformation produced a layer-parallel S_1 foliation and tight to isoclinal F_1 folds, which are overprinted by a regionally pervasive and penetrative, northeast-trending S_2 transposition fabric that is axial planar to upright, tight to isoclinal F_2 folds that plunge steeply east. The geometry and configuration of the principal sulphide lenses, coupled with mesoscopic deformation structures in the hostrocks, indicate that the Ruttan deposit is overprinted by previously unrecognized, macroscopic F_2 folds that define the north limb of a map-scale, downward-facing F_2 syncline. The D_3 deformation produced a northeast-trending, anastomosed network of ductile shear zones in the mine, which include the North Wall Shear Zone (NWSZ), Art's Shear Zone (ASZ) and the East Shear Zone (ESZ). Asymmetric S_3 fabrics are ubiquitous and consistently record dextral transcurrent shear, with a variable component of normal oblique slip. The D_2 and D_3 deformations are manifested in the macroscopic distribution and geometry of the major orebodies: the B lenses are disposed in a train of lenticular, steeply plunging ore shoots along the trace of the D_3 NWSZ and exhibit evidence of back rotation in a kinematic regime of dextral shear. The D, J and JS lenses define a stacked series of tight to isoclinal closures along the southern hinge of a macroscopic, Z-asymmetric F_2 fold, which is transected and displaced by the ESZ and ASZ. The D_4 deformation structures are only locally observed in the mine and consist of discrete, ductile shear zones that dip shallowly south and record south-over-north (thrust-sense) shear. These structures apparently had little influence on the deposit geometry.

The timing and tectonic significance of these deformations are constrained by the Brehaut Lake granodiorite pluton, which intrudes the Ruttan deposit from the west and stitches the tectonostratigraphic succession. Contact metamorphism in the thermal aureole of this pluton produced spectacular, lower amphibolite facies, metamorphic mineral assemblages in hydrothermally altered rocks of the MSU. Evidence of late-kinematic annealing recrystallization, porphyroblastesis and granodiorite dike emplacement in D_3 shear zones constrain pluton emplacement to the latest stages of the tectonothermal history. A sample from a late-tectonic granodiorite dike in the West mine yielded a concordant U-Pb zircon age of 1852.5 ±1.2 Ma, as well as three variably discordant $^{207}Pb/^{206}Pb$ ages of approximately 1857–1865 Ma. These data indicate ca. 1.865–1.852 Ga emplacement of the Brehaut Lake pluton, roughly coeval with ca. 1.87–1.85 Ga successor-arc magmatism along the north margin of the Trans-Hudson Orogen.

The ca. 1.88–1.85 Ga tectonic history of the Rusty Lake belt appears to be closely analogous to that of the well-documented Amisk collage along the southeast margin of the Trans-Hudson Orogen. The D_1 deformation is interpreted to record ca. 1.88–1.87 Ga tectonic assembly of the Ruttan mine tectonostratigraphy into an intraoceanic structural collage along the northwest margin of the Trans-Hudson Orogen, closely followed by continued or renewed shortening of the D_1 structural architecture during D_2 deformation, perhaps as a consequence of accretion of the structural collage to the south margin of the Archean Hearne craton. The geometry and kinematics of the regionally extensive D_3 shear-zone network indicate orogen-scale east-west shortening of the structural collage, roughly coeval with ca. 1.87–1.85 Ga successor-arc magmatism. It is speculated that the apparently solitary Fox Lake and Ruttan VMS deposits may be segments of a single VMS system, which was displaced during east-west shortening of the Trans-Hudson Orogen and large-scale, left-lateral movement on a northwest-trending, crustal-scale break that is manifested as the Johnson and Vol faults.

The structural framework presented in this report provides a greatly improved context in which to understand the stratigraphy and genesis of the Ruttan deposit. In the context of this framework, several potential models for primary deposition and syntectonic remobilization of sulphide are proposed to explain the style, geometry and distribution of the most significant orebodies in the Ruttan deposit. These models provide important constraints for ongoing studies of rare-earth-element (REE) and trace-element systematics in the Ruttan VMS system, as well as practical empirical exploration criteria that can be utilized to formulate exploration strategies and assess the residual VMS potential on local to regional scales in the Rusty Lake belt.

TABLE OF CONTENTS

TABLES

Page

FIGURES

Introduction

The giant Ruttan volcanogenic massive sulphide (VMS) deposit, located 21 km east of the town of Leaf Rapids in northwestern Manitoba (Figure 1), is among the largest known VMS deposits in the world, with an estimated preproduction geological resource of 82.8 million tonnes grading 1.37 wt.% Cu, 1.63 wt.% Zn, 0.08 wt.% Pb, 0.49 g/t Au and 13.11 g/t Ag (Barrie and Taylor, 2001). Hosted by Paleoproterozoic metavolcanic rocks of the Rusty Lake belt in the Trans-Hudson Orogen, the deposit was discovered in 1969 by Sherritt Gordon Mines Ltd. and brought into production in 1973. The Ruttan mine was acquired in 1987 by Hudson Bay Mining and Smelting Co., Limited, and recorded 29 years of nearly continuous production from open pit (1973–1980) and underground (1979–2002) operations. During this time interval, the mine produced roughly 62 million tonnes of sulphide ore with an average grade of 1.2 wt.% Cu, 1.5 wt.% Zn, 0.5 g/t Au and 12.2 g/t Ag (Barrie and Taylor, 2001). Due to low commodity prices and dwindling ore reserves, the Ruttan mine was permanently closed in July 2002.

This study was initiated in 2002 by the Manitoba Geological Survey as part of an ongoing geoscience initiative in the Lynn Lake–Leaf Rapids region. In cooperation with the Geological Survey of Canada, one aspect of this initiative involves updating and integrating the stratigraphy, structure, geochemistry and geochronology of the Rusty Lake belt and the giant, though apparently solitary, Ruttan deposit. Given that giant VMS deposits rarely occur in isolation, emphasis has been placed on establishing practical new geochemical (e.g., Gale et al., 2002) and structural criteria to evaluate the residual mineral potential of the Ruttan mine area. It is hoped that this information, in conjunction with the results of concurrent regional-scale geoscience programs (e.g., Beaumont-Smith and Böhm, 2002; Corrigan and Rayner, 2002; Gale and McClenaghan, 2002), will stimulate exploration activity in the highly prospective, though relatively underexplored, Lynn Lake–Leaf Rapids region.

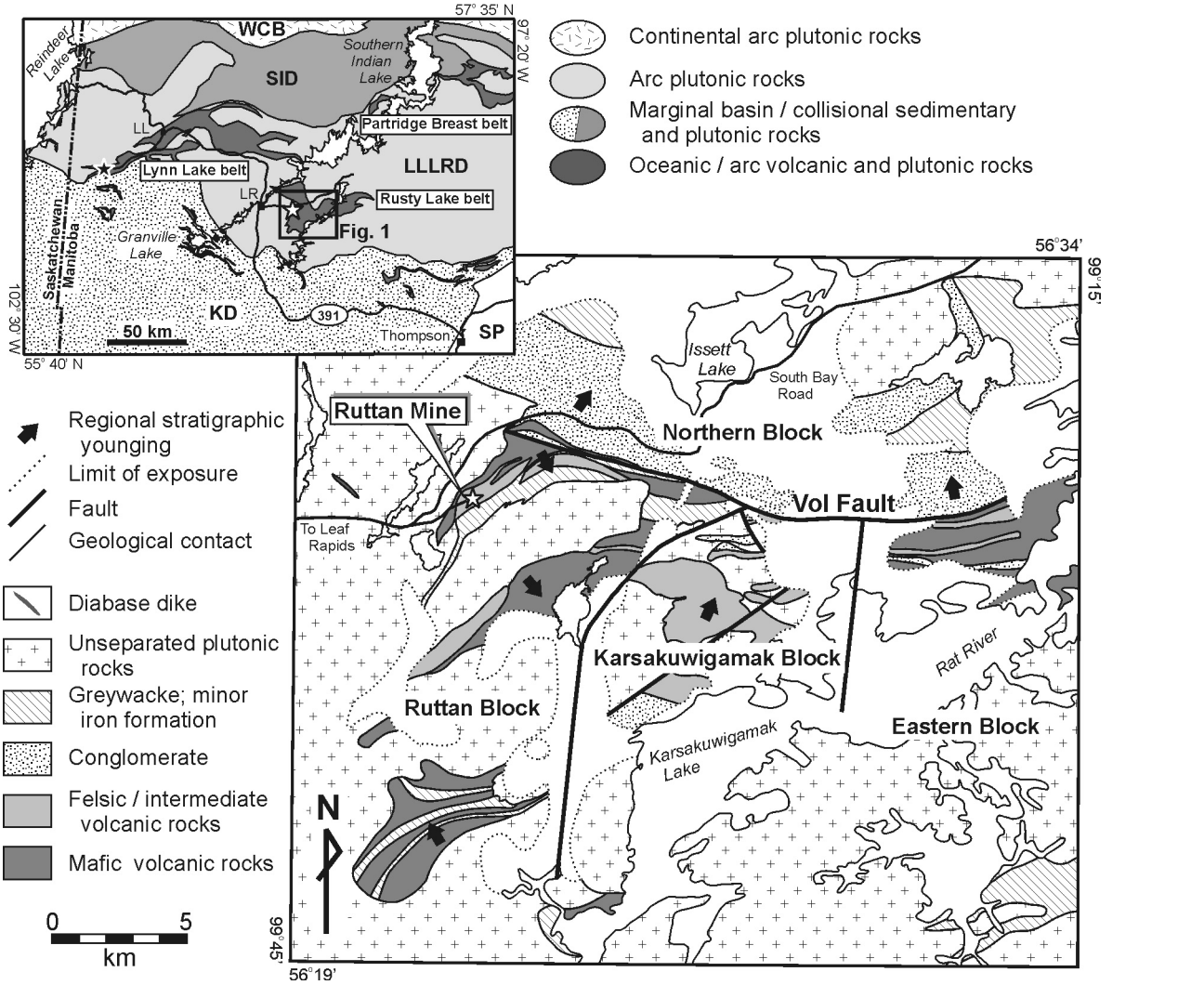

Figure 1: *Simplified geology of the southwest Rusty Lake belt (*after *Baldwin, 1988), showing the location of the Ruttan deposit. Inset map shows the regional setting of the Rusty Lake belt on the north flank of the Trans-Hudson Orogen in northwestern Manitoba (the locations of the Ruttan and Fox Lake mines are indicated by the white and black stars, respectively). Abbreviations: KD, Kisseynew Domain; LL, Lynn Lake; LR, Leaf Rapids; LLLRD, Lynn Lake–Leaf Rapids Domain; SID, Southern Indian Domain; SP, Superior Province; WCB, Wathaman-Chipewyan Batholith.*

Background

The geology of the Ruttan deposit (Figure 2) has been described by Speakman et al. (1982), Ames et al. (1990), Ames (1991), Ames and Scoates (1992), Ames (1996), Ames and Taylor (1996), and Barrie and Taylor (2001). Although all of these authors provided brief descriptions of apparently complex, multiphase deformation structure, the structural geology of the deposit has never been documented in detail, and the influence of structure with respect to the spatial configuration and geometry of the sulphide orebodies was poorly understood. As previous investigators note, the Ruttan orebodies are prominently elongate and plunge to the southeast at moderate to steep angles (Figure 3). The long axes of the orebodies are subparallel to mineral and intersection lineations in the hostrocks, the hinges of mesoscopic isoclinal folds, and the β-axis of a late network of anastomosed shear zones (e.g., Speakman et al., 1982; Reid, 1995; Ames and Taylor, 1996), suggesting a number of possible structural explanations for their elongate aspect (i.e., a structural control). The level plans and structural descriptions of Speakman et al. (1982) indicate that the spatial configuration of the orebodies is, at the very least, significantly influenced by the late shear zones (e.g., Ames and Taylor, 1996; Schwartz and Brown, 2000).

Nevertheless, recent stratigraphic and genetic models for the Ruttan deposit effectively disregard the possibility of structural control and are predicated on the assumption that the orebody geometry is a direct manifestation of primary depositional processes. Barrie and Taylor (2001), for example, suggested that the elongate aspect and local extreme thickness of the Ruttan orebodies indicate sulphide deposition in a half-graben setting, controlled by synvolcanic growth faults. Although they noted that the thickest sulphide intervals are comparable to the structurally thickened portions of other giant VMS deposits, they did not examine this possibility for

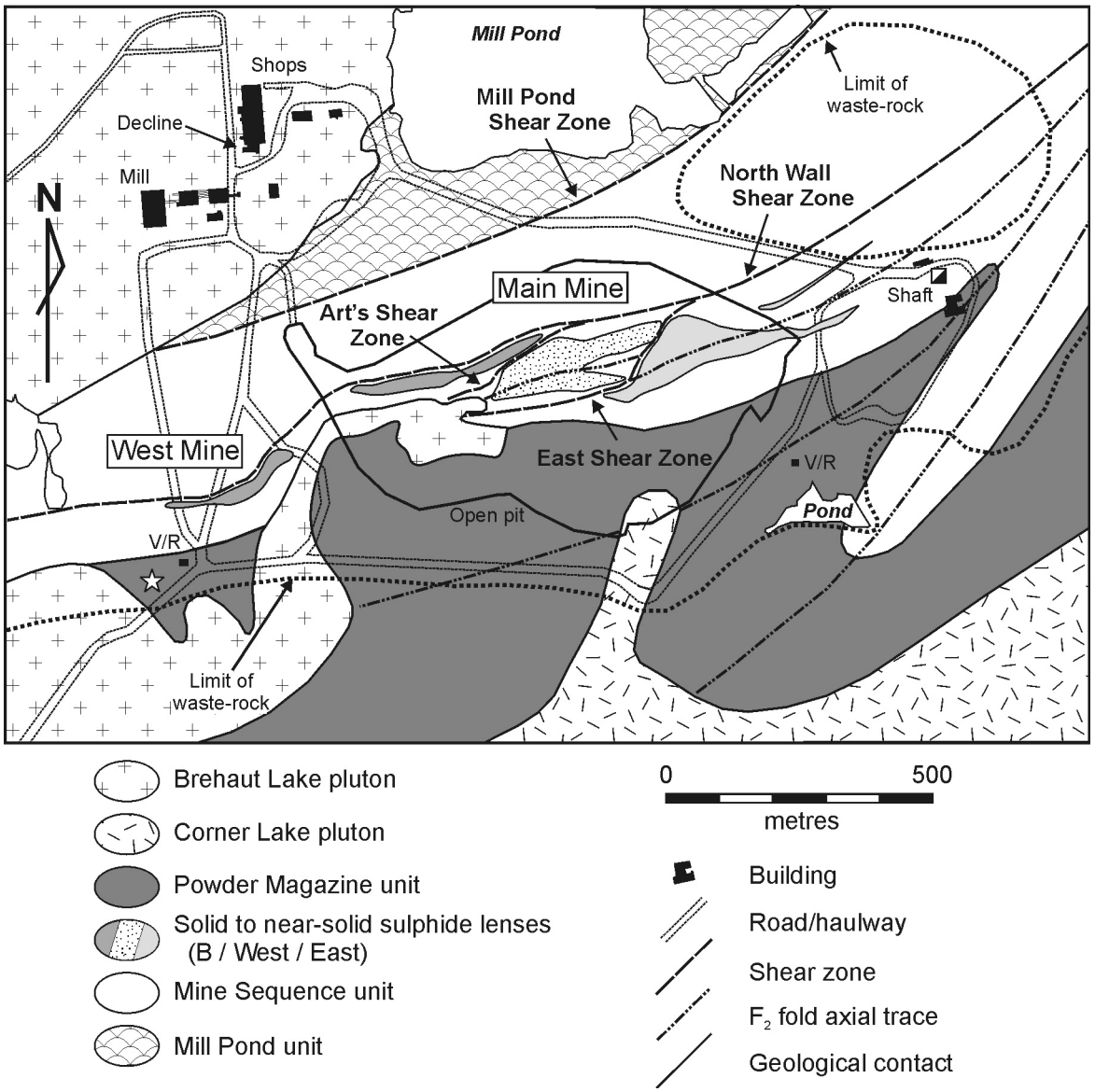

Figure 2: *Geology of the Ruttan mine area (*after *Ames and Scoates, 1992), showing a simplified three-fold subdivision of the supracrustal rocks, as well as the major structural features. The star indicates the location of the outcrop shown in Figure 4. Abbreviations: V/R, vent raise.*

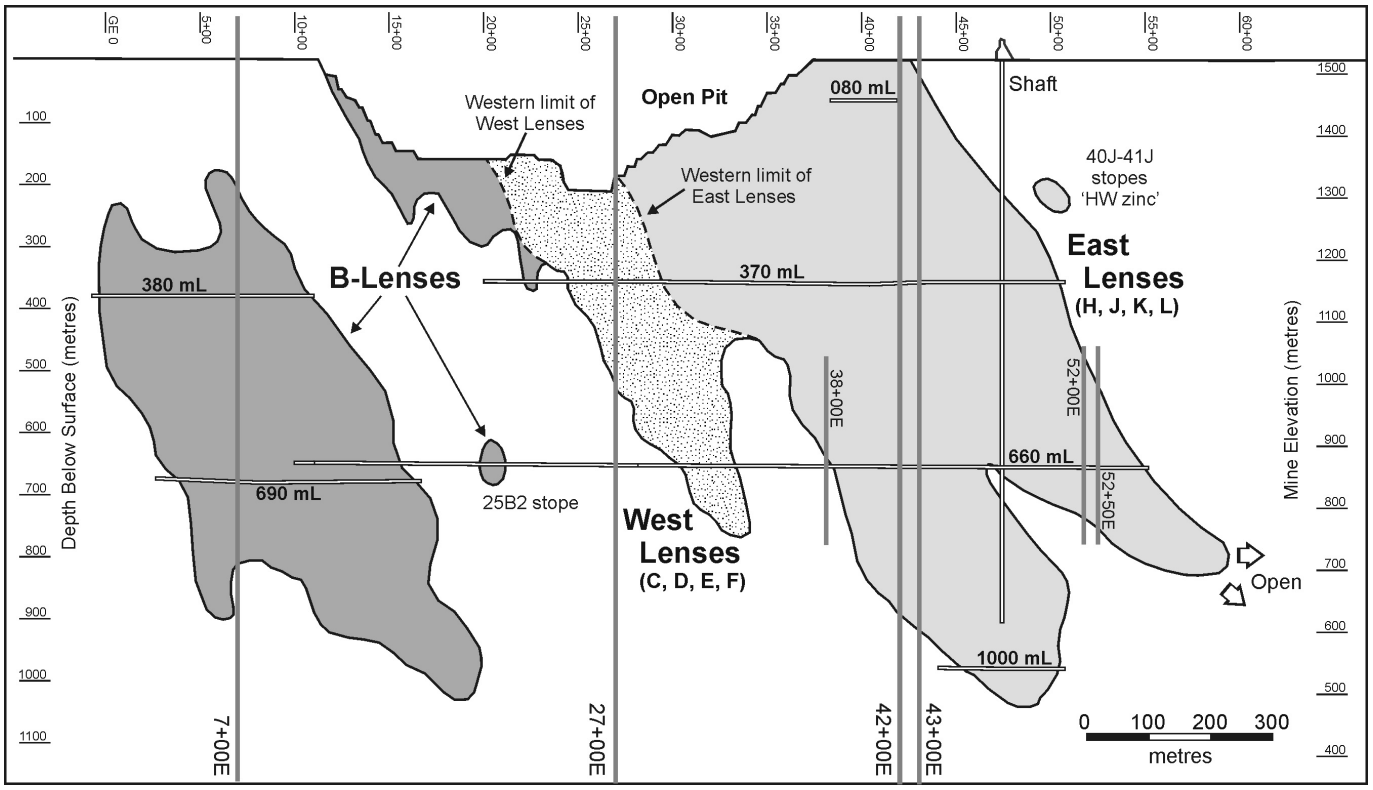

Figure 3: *Simplified vertical longitudinal section of the Ruttan deposit, looking north-northwest, showing the locations of the level plans and sections cited in the text. The fill patterns for the sulphide lenses correspond to those in Figure 2.*

the Ruttan deposit, and the inferred growth faults are traced in a linear manner across several well-documented, late-tectonic shear zones. Similar genetic models have traditionally been advocated by company geologists (R. Yaworski, pers. comm., 2002) and have significantly influenced conceptual exploration in the mine area. As described in this report, however, such models perpetuate an overly simplistic view of the deposit geology that is impractical for the purpose of geological modelling.

Purpose and methods

In this context, the present study was initiated to gain a better understanding of the structural geology, deformation history and geometry of the Ruttan deposit. The purpose of this study is to

1) provide an explanation for the spatial configuration and geometry of the known sulphide orebodies, and evaluate whether the application of a structure-based model could serve to highlight areas with exploration potential;
2) provide an improved stratigraphic context for ongoing detailed geochemical mapping programs and exploration-potential assessments in the mine area; and
3) produce a summary report that will document some salient aspects of the structural geology of the Ruttan deposit, as understood at mine closure.

This report provides a general summary of observations pertaining to the structural geology of the Ruttan deposit, based on 16 days of underground fieldwork, coupled with a thorough review of published research and unpublished company reports and data. Due to the very large size of the deposit, the time constraints on underground access, and the logistical considerations associated with working underground, the fieldwork focused on documenting the style, geometry and sequence of mesoscopic deformation structures at widely distributed sites in the Main and West mines (Figure 2). This work was greatly facilitated by mine geology staff, who accompanied the authors underground at all times and provided a wealth of first-hand information on the deposit geology as collected during years of detailed observation. The staff also provided free access to drillhole sections and logs, geological level plans and ore-shell models, all of which were incorporated into this study. Surface exposures were examined by the first author over the course of two days, and a particularly informative outcrop in the hangingwall of the West mine was mapped in detail. The first author also spent two weeks examining drillcore, with emphasis on relogging select drillholes from key localities identified underground.

Regional geological setting

The Ruttan VMS deposit is situated in the west-central portion of the Paleoproterozoic Rusty Lake belt in the Lynn Lake–Leaf Rapids Domain, on the northern flank of the Trans-Hudson Orogen in northwestern Manitoba (Figure 1). Contrasts in rock types and apparent stratigraphic discontinuities prompted Baldwin (1980, 1988) to subdivide the metavolcanic

and metasedimentary rocks of the Rusty Lake belt into four fault-bounded blocks. The Ruttan deposit is located in the northwest portion of the Ruttan Block, which consists mainly of submarine mafic metavolcanic and metasedimentary rocks that are disposed in three northeast-trending panels, separated by large composite plutons. The Ruttan Block is bounded to the west and south by granitoid plutons, and to the east by subaerial felsic metavolcanic rocks of the Karsakuwigamak Block. Northeast-trending map units in the Ruttan Block are truncated to the north by the regional-scale Vol Fault (Ames, 1996) and are juxtaposed with submarine metasedimentary rocks of the Northern Block (Figure 1). Regional-scale isoclinal folds are indicated by map patterns and younging reversals in the Ruttan and Northern blocks (Baldwin, 1988), and appear to predate the latest increment of movement along the Vol Fault. Metamorphic mineral assemblages in the southwest Rusty Lake belt indicate greenschist-facies regional metamorphism, although middle-amphibolite-facies assemblages are present on the margins of the belt and adjacent to granitoid plutons (Baldwin, 1988). In the interest of brevity, the prefix 'meta' is omitted from rock names in this report.

Recent U-Pb geochronology by Rayner and Corrigan (2004) indicates that epiclastic rocks in the Ruttan Block contain detrital zircons of exclusively volcanic provenance, with most yielding ages within error of the typical age range (i.e., 1.91–1.88 Ga) of oceanic volcanism in the Trans-Hudson Orogen (e.g., Baldwin et al., 1987; Gordon et al., 1990; Stern et al., 1995, 1999; Lucas et al., 1996). A sample of quartz-porphyritic rhyolite collected from the hangingwall of the Ruttan deposit yielded a U-Pb zircon age of 1883 ±2 Ma, which Rayner and Corrigan (2004) interpreted as the probable minimum age for volcanism in the Ruttan mine sequence. These data are compatible with the 1878 ±3 Ma U-Pb zircon age reported by Baldwin et al. (1987) for a rhyolite flow in the upper stratigraphic level of the Karsakuwigamak Block, which was the only previous age constraint on volcanism in the Rusty Lake belt. Collectively, these data indicate that volcanism in the Rusty Lake belt likely spanned the 1.91–1.88 Ga time interval and suggest that the Ruttan deposit is of similar age to VMS deposits in the Flin Flon–Snow Lake belt (e.g., Stern et al., 1995, 1999) and the Lynn Lake belt (e.g., Beaumont-Smith and Böhm, 2002, 2003).

Local geological setting of the deposit

Stratigraphy

The geology and stratigraphy of the Ruttan mine area are described in detail by Jackson (1979), Speakman et al. (1982), Ames (1996) and Ames and Taylor (1996), and were mapped at 1:5000 scale by Ames and Scoates (1992). For the purpose of this report, the supracrustal rocks in the immediate mine area are divided into the Mill Pond unit, Mine Sequence unit (MSU) and Powder Magazine unit, from north to south respectively (Figure 2). These units generally trend east-northeast and dip steeply to the south-southeast. The Mill Pond unit consists of ocean-floor mafic volcanic rocks (Ames, 1996) that are juxtaposed to the south across the northeast-trending Mill Pond Shear Zone with the MSU (Figure 2). Based on distinct differences in geochemistry, stratigraphy, structure and alteration across this shear zone, Ames (1996) suggested that the Mill Pond unit is probably allochthonous with respect to the MSU. The Mill Pond Shear Zone is stitched by the Brehaut Lake pluton (Figure 2).

The MSU is subdivided into three distinct lithological sections (Ames, 1996). The northern section comprises a homogeneous package of layered, heterolithic, intermediate volcaniclastic rocks that ranges from 200 to 300 m thick and is known in mine terminology as the 'footwall volcaniclastic rocks'. The middle section of the MSU, which is approximately 75 m thick, consists of variably altered volcaniclastic and fragmental-volcanic rocks of dacitic and rhyolitic composition (Ames, 1996). This section includes several large lenses of solid to near-solid sulphide that collectively constitute the Ruttan VMS deposit and are described in detail below. A distinctive package of light grey to white, quartz-phyric, rhyolitic volcaniclastic rocks defines the southern section of the MSU and ranges up to 100 m thick. This section corresponds to the 'upper felsic volcaniclastic unit' of Ames (1996) and is the source of the 1883 ±2 Ma U-Pb age obtained by Rayner and Corrigan (2004). Preliminary lithogeochemistry by Ames (1996) indicated that the MSU is of transitional calcalkalic to tholeiitic affinity.

This study made no attempt to further subdivide the stratigraphy of the MSU, and the compilation maps and sections in this report show only the principal lenses of solid and near-solid sulphide. In the absence of marker horizons in the central portion of the MSU, the sulphide lenses were found to be the only laterally extensive, consistently identifiable units in the often poor-quality exposures underground. The spatial configuration of the sulphide lenses provides important, first-order insights into the macroscopic structure of the deposit. In addition, patterns of metal zoning and style of mineralization within individual lenses locally appear to provide a reliable indication of younging direction, and thus some insight into the stratigraphy of the MSU. This aspect is particularly important, as the combined effects of intense hydrothermal alteration, penetrative deformation, and thorough metamorphic recrystallization have obscured or destroyed primary features in the central MSU, which contains few convincing examples of primary layering and is apparently devoid of younging criteria.

To the south, the MSU is overlain by intercalated greywacke-mudstone turbidite and polymictic conglomerate of the Powder Magazine unit, along what has traditionally been regarded as a conformable stratigraphic contact (e.g., Speakman et al., 1982; Baldwin, 1988; Ames, 1996; Ames and Taylor, 1996; Barrie and Taylor, 2001; Gale, 2003). However, in the single location where the authors were able to directly examine this contact (in the 29 pillar crosscut on the MM490mL level), the Powder Magazine unit lies in direct contact with the major hangingwall sulphide lens in the MSU. In this location, the 'upper felsic volcaniclastic unit' of Ames (1996) is absent and the Powder Magazine unit contains a prominent centimetre-scale layering that is markedly discordant with, and truncated by, the upper contact of the sulphide lens. A similar

relationship is evident on surface, 2.0 km northeast of the open pit, in a location where Ames (1996) described a conformable contact relationship. As mapped by Ames and Scoates (1992), however, the contact in this location cuts obliquely across the section of the Powder Magazine unit and is discordant with bedding (*see also* Ames, 1996, Figure 3a). These observations indicate that the contact is either tectonically modified or wholly tectonic. Regarding to the latter possibility, it may be significant that a U-Pb geochronological analysis of the detrital zircon population in the Powder Magazine unit did not identify any Archean zircons (Rayner and Corrigan, 2004), in sharp contrast to massive dacite in the underlying MSU, in which Archean xenocrysts appear to be abundant (Ames et al., 2002). These data are interpreted to indicate that the Powder Magazine unit was not derived through erosion of the immediately underlying MSU.

Structural overview

In the mine area, the supracrustal rocks typically exhibit coarse recrystallized textures and penetrative schistose or gneissic fabrics. Based on the descriptions of previous workers (e.g., Baldwin, 1988; Ames, 1996), it would appear that these rocks record significantly higher finite strain than is typical of the region, most likely as a consequence of strain being partitioned into the rheologically weak sulphide lenses and altered hostrocks during regional deformation (e.g., Speakman et al., 1982). Overprinting relationships exhibited by mesoscopic deformation structures in the hostrocks suggest a multiphase sequence of ductile deformation. Recognition of this structural complexity is critical to understanding the geology and geometry of the Ruttan deposit, and the salient structural features are briefly summarized here to provide context for the descriptions that follow. Deformation structures in the hostrocks are described in detail in a later section, with emphasis on the critical overprinting relationships that were used to reconstruct the sequence of deformation.

As noted by Speakman et al. (1982), the structural style in the Ruttan mine area is dominated by isoclinal folding, which is here assigned to the F_2 generation on the basis of observed overprinting relationships with an earlier generation of planar fabric (S_1). Mesoscopic examples of these folds are abundant in the MSU and at least the northern portion of the Powder Magazine unit (Figure 4), and are characteristically rootless and intrafolial with respect to transposed layering and a regional, east-northeast-trending transposition foliation (S_2) that parallel the mine trend. Evidence of strongly partitioned transposition is observed on several scales, but is most prominently manifested in metre- to decimetre-scale domains of relatively low finite strain, in which primary textures are locally preserved and an early, centimetre- to metre-scale layering, which may represent either primary bedding or an early tectonite fabric, is oriented orthogonal to the mine trend (Figure 5a). These domains define the hinges of meso- and macroscopic isoclinal F_2 folds, the limbs of which are transposed into concordance with the mine trend. As shown in Figure 2, these criteria have been used, in conjunction with map patterns and mesoscopic deformation structures, to define several macroscopic F_2 folds in the mine area that were previously unrecognized.

The F_2 folds and fabrics are overprinted by a network of anastomosed ductile shear zones that are attributed to D_3

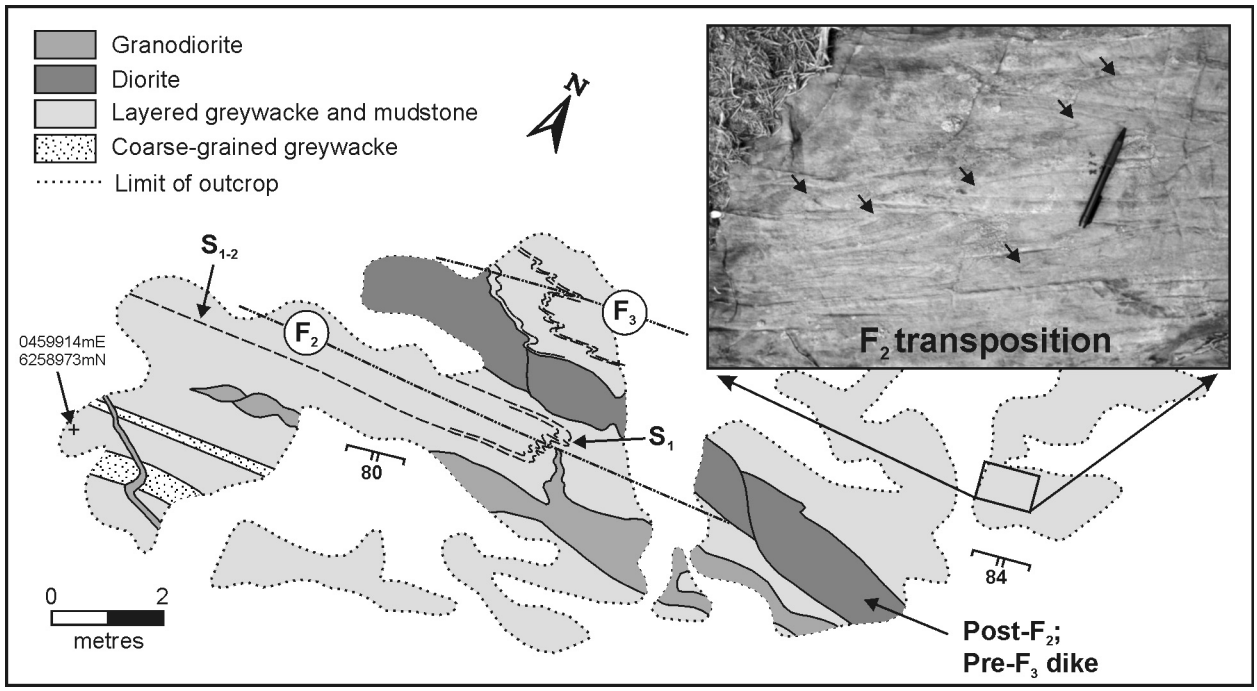

Figure 4: *Detailed sketch map of an outcrop in the immediate hangingwall of the West mine, Ruttan deposit, which neatly summarizes the observed overprinting relationships among various generations of deformation structures and intrusive rocks near the north contact of the Powder Magazine unit. The outcrop location is indicated by the UTM coordinates (NAD 83, Zone 14) and is shown by the star on Figure 2. Inset photograph illustrates tight to isoclinal, rootless F_2 fold closures defined by transposed layers in the Powder Magazine unit.*

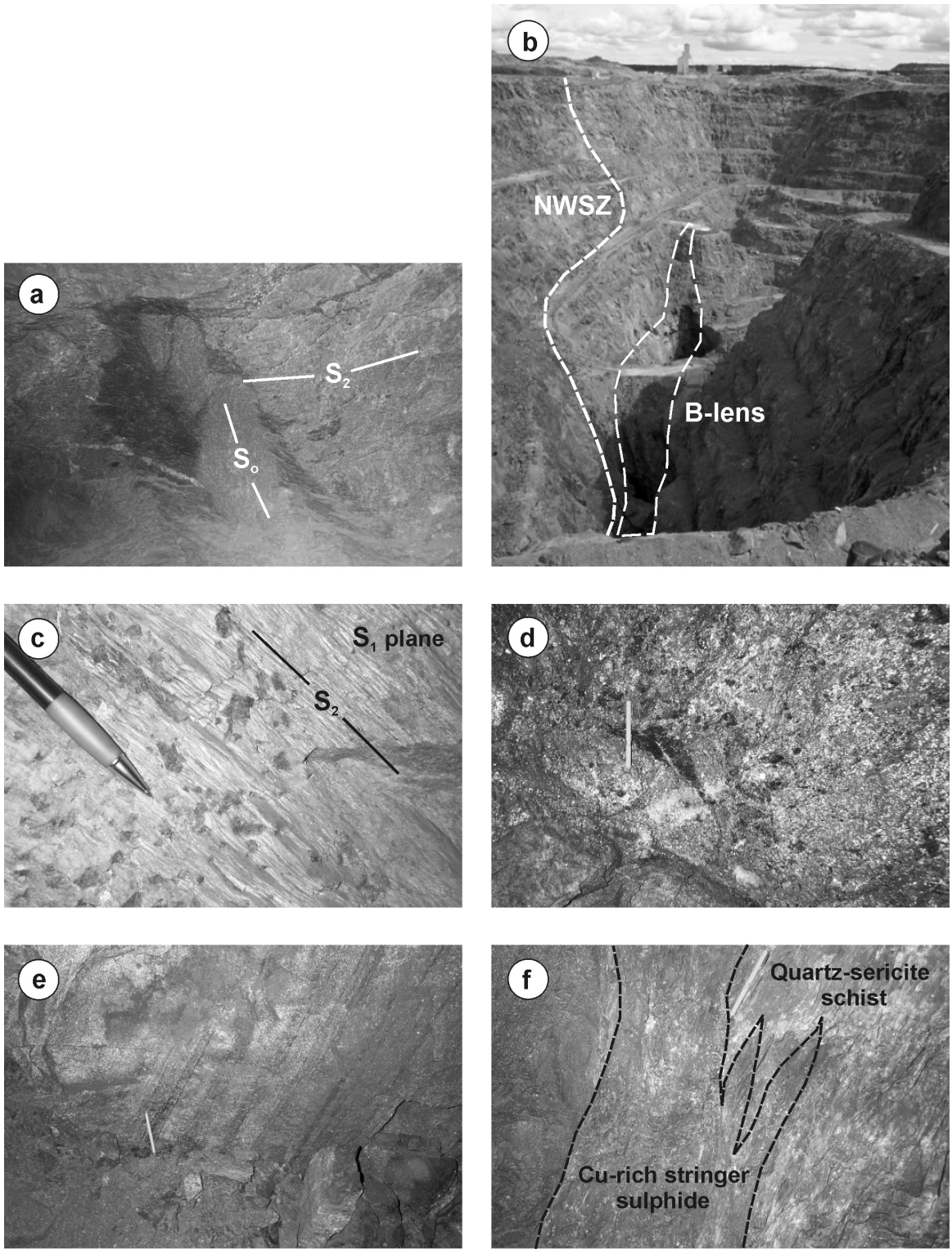

Figure 5: *Photographs of structural features and sulphide ores from the Ruttan deposit:* ***a)*** *metre-scale layering (S_o) in the Mine Sequence unit (field of view ~3 m), showing an orthogonal relationship to the regional S_2 fabric in the hinge of an F_2 fold, back exposure (facing north), 30 m southwest of the refuge station, level MM660mL;* ***b)*** *Ruttan open pit, looking east from the main ramp (headframe in distance for scale), heavy dashed line indicating the trace of the North Wall Shear Zone in the immediate footwall of the B lens (thin dashed line and open stopes);* ***c)*** *S_1-S_2 crenulation fabric overgrown by late-kinematic staurolite porphyroblasts in sericite-quartz schist, wall exposure (facing northeast), level MM370mL, east footwall drift;* ***d)*** *copper-rich massive ore at the base of the B lens, wall exposure (facing north), level WM280mL, 9B2 stope (pencil for scale);* ***e)*** *zinc-rich layered ore with rhythmic layering of sphalerite (dark) and pyrite (light) at the top of the JS lens, wall exposure (facing west), level MM800mL, 37J1 stope (pencil for scale);* ***f)*** *copper-rich stringer ore at the base of the JS lens, wall exposure, facing west, level MM800mL, 37J1 stope (pencil for scale).*

deformation. Speakman et al. (1982) defined three principal shear zones in the mine (Figure 2): the North Wall Shear Zone (NWSZ), Art's Shear Zone (ASZ) and the East Shear Zone (ESZ). The ASZ and ESZ are sigmoidal structures that dip toward the southeast at steep to moderate angles and appear to splay off the hangingwall of the steeply south-southeast-dipping NWSZ (Figure 2). These shear zones are marked by laterally continuous zones of strongly foliated chlorite-biotite schist that range up to 30 m in thickness. Asymmetric fabrics are ubiquitous and consistently indicate dextral shear, with a variable component of normal oblique slip. As indicated by Speakman et al. (1982) and Ames and Scoates (1992), the NWSZ defines the immediate footwall of the deposit in the west portion of the Main mine (Figure 2). This relationship is clearly evident in the north wall of the open pit, where weakly altered 'footwall volcaniclastic rocks' below the NWSZ define the footwall of open stopes on the B lens (Figure 5b). Although Ames and Scoates (1992) indicated that the NWSZ and the B lens diverge west of the open pit, level plans of the West mine also consistently indicate 'footwall volcaniclastic rocks' in the immediate footwall of the lens. On these plans, southeast-trending granodiorite dikes up to 20 m thick are locally mapped continuously upward through the footwall of the B lens, but abruptly terminate at the footwall contact. Strongly foliated chlorite-biotite schist envelops the B lens and contains disrupted and boudinaged granodiorite dikes (Ames and Taylor, 1996). These observations are interpreted to indicate that the NWSZ also defines the immediate footwall of, and partially envelops, the B lens in the West mine (Figure 2).

Plutonic rocks

To the west and north of the Ruttan deposit (Figure 2), the supracrustal section is truncated by the Brehaut Lake pluton, which consists primarily of homogeneous, light grey, medium-grained biotite granodiorite. The margin of the pluton west of the deposit is marked by a wide zone of granodiorite intrusion breccia (Baldwin, 1988; Ames, 1996). Granodiorite dikes locally constitute more than 50% of the section in the West mine. These dikes decrease in abundance to the east and are only locally observed in the extreme western portion of the Main mine. To the south, the supracrustal rocks are intruded by the Corner Lake pluton (Figure 2), which, in the immediate mine area, consists mainly of dark green, fine- to medium-grained hornblende diorite. Preliminary lithogeochemistry by Ames (1996) indicated that the Corner Lake and Brehaut Lake plutons are metaluminous, moderately potassic, calcalkaline volcanic-arc plutons and are thus chemically similar to the 'successor-arc' plutons described by Whalen et al. (1999) from the Flin Flon Belt. Dikes and sills of fine- to medium-grained mafic intrusive rock are abundant throughout the deposit, and over-printing and crosscutting relationships indicate multiple generations of mafic magmatism, ranging from pre- to post-tectonic. The footwall of the deposit contains a distinctive swarm of light grey, aphanitic to weakly feldspar-phyric felsic dikes that are typically observed in the central portions of late ductile shear zones and are strongly foliated.

U-Pb geochronology of the Brehaut Lake pluton

In an effort to constrain the age of the Brehaut Lake pluton, a 30 kg sample of visually unaltered and undeformed, homogeneous granodiorite was collected for U-Pb geochronological analysis. The sample was collected from an irregular, approximately 20 m thick dike that sharply crosscuts hydrothermal alteration and deformation structures in the footwall of the B lens in the West mine (level 440mL, 4B2 stope, east draw-point) and is presumed to be comagmatic with the adjacent Brehaut Lake granodiorite pluton.

U-Pb analytical methods

Conventional U-Pb dating of zircon by isotope-dilution, thermal-ionization mass spectrometry was completed at the University of Alberta Radiogenic Isotope Facility in Edmonton, Alberta, and generally follows the procedures outlined in Heaman et al. (2002). All analyses were performed on a VG354 mass spectrometer operated in single Faraday or Daly (analogue) collector peak-hopping mode, and were corrected for mass discrimination (0.088%/amu Pb; 0.155%/amu U) based on replicate measurement of the NBS981 and U500 standards. In addition, all measurements obtained with the Daly photo-multiplier detector were adjusted for detector bias (0.13%/amu Pb; 0.15%/amu U). The isotopic composition of common Pb in excess of analytical blank (2 pg Pb) was calculated using the two-stage model of Stacey and Kramers (1975). All errors reported in Table 1 are quoted at 1σ and were calculated by numerical propagation of all known sources of uncertainty.

Table 1: U-Pb zircon analytical data from the granodiorite dike on level WM440mL, 4B2 stope, Ruttan deposit.

Zircon	Description	Wt. (mg)	U (ppm)	Pb rad. (ppm)	^{204}Pb (pg)	Model Th/U	Isotopic ratios			Age (Ma)			% disc.
							^{207}Pb/^{235}U	^{206}Pb/^{238}U	^{207}Pb/^{206}Pb	^{206}Pb/^{238}U	^{207}Pb/^{235}U	^{207}Pb/^{206}Pb	
Z1	sp eh co na	6.0	425.4	145.4	11.9	0.27	5.2007	0.33300	0.11327	1852.9 ±2.3	1852.7 ±1.2	1852.5 ±0.6	0
Z3	sp sh lt ab	3.6	486.6	167.6	12.5	0.31	5.2164	0.33177	0.11403	1846.9 ±2.3	1855.3 ±1.2	1864.7 ±0.8	1.1
Z4	is pl sh lt ab	5.0	260.2	90.5	4.1	0.36	5.1799	0.33092	0.11353	1842.8 ±2.2	1849.3 ±1.2	1856.6 ±0.9	0.9
Z5	eq pl sh co ab	1.3	217.2	77.0	4.4	0.34	5.3174	0.33901	0.11376	1881.9 ±2.8	1871.7 ±2.3	1860.3 ±3.4	-1.3

Abbreviations: ab, abraded; co, colourless; eh, euhedral; eq, equant; is, isometric; lt, light tan; na, nonabraded; pl, platy; sp, short prismatic; sh, subhedral.

The error ellipses are shown at 2σ on the concordia diagram (Figure 6).

U-Pb analytical results

The least magnetic mineral fractions from the granodiorite sample yielded abundant colourless to light tan, euhedral to subhedral, dominantly short prismatic to equant zircon crystals of variable quality. Thirty of the larger (>80 μm in longest dimension), best quality zircons were abraded and, from these, three single crystals were selected for U-Pb isotope analysis (zircons 3, 4 and 5). Also selected for analysis was a euhedral tip that was broken off a large, colourless, short-prismatic, nonabraded zircon crystal (zircon 1).

All analyzed zircons exhibit similar U concentrations and Th/U ratios (Table 1), suggesting a similar paragenesis. Zircon 1 yielded a concordant age of 1852.5 ±1.2 Ma (Figure 6), which is interpreted to indicate the emplacement age of the dike, whereas the three abraded zircons yielded slightly older and variably discordant $^{207}Pb/^{206}Pb$ ages of approximately 1857–1865 Ma, indicating the presence of inherited components of slightly older age. These data are interpreted to indicate that emplacement of the Brehaut Lake pluton occurred between ca. 1.865 and 1.852 Ga, and was thus coeval with ca. 1.87–1.85 Ga successor-arc and continental-arc magmatism (Bickford et al., 1990) along the northern margin of the Trans-Hudson Orogen. The significance of these data with respect to deformation timing is addressed in the 'Discussion' section.

Alteration and metamorphism

In proximity to sulphide mineralization, hydrothermal alteration effects are pervasive and locally intense in the central portion of the MSU, and are generally manifested as interleaved, lenticular zones of silicification, chloritization and sericitization. These rocks locally contain spectacular metamorphic mineral assemblages and thus provide important constraints on the relative timing of deformation and metamorphism in the mine area (e.g., Speakman et al., 1982; Ames, 1996; Ames and Taylor, 1996). In general, two mineral assemblages predominate: 1) chlorite-biotite ± plagioclase, garnet, anthophyllite, cordierite, actinolite, talc, magnetite, quartz or pyrite, and; 2) sericite-quartz ± biotite, plagioclase, staurolite, andalusite, cordierite, gahnite or pyrite. The chlorite-biotite assemblage is common throughout the deposit in both the footwall and hangingwall to the sulphide mineralization, whereas the sericite-quartz assemblage is only extensively developed in the eastern Main mine, where it appears to be largely bounded by the NWSZ and the structurally highest sulphide lens. Staurolite, andalusite, garnet, cordierite and anthophyllite form coarse (0.5–5 cm) idioblastic porphyroblasts that are clearly late kinematic with respect to fabrics in the chlorite or sericite schist matrix (Figure 5c).

In the deeper levels of the West mine, the predominant metamorphic assemblage is biotite-chlorite-anthophyllite-cordierite-garnet, which locally contains spectacular radiating masses of acicular anthophyllite up to 20 cm across. Close to the eastern contact of the Brehaut Lake pluton, these porphyroblasts overgrow a granoblastic and isotropic, coarse-grained matrix of biotite, cordierite and chlorite. As described by Ames and Taylor (1996), these metamorphic mineral assemblages indicate peak metamorphism in the lower amphibolite facies (500–600°C, 3–4 kb), which is significantly higher than the lower greenschist-facies metamorphism observed on a regional

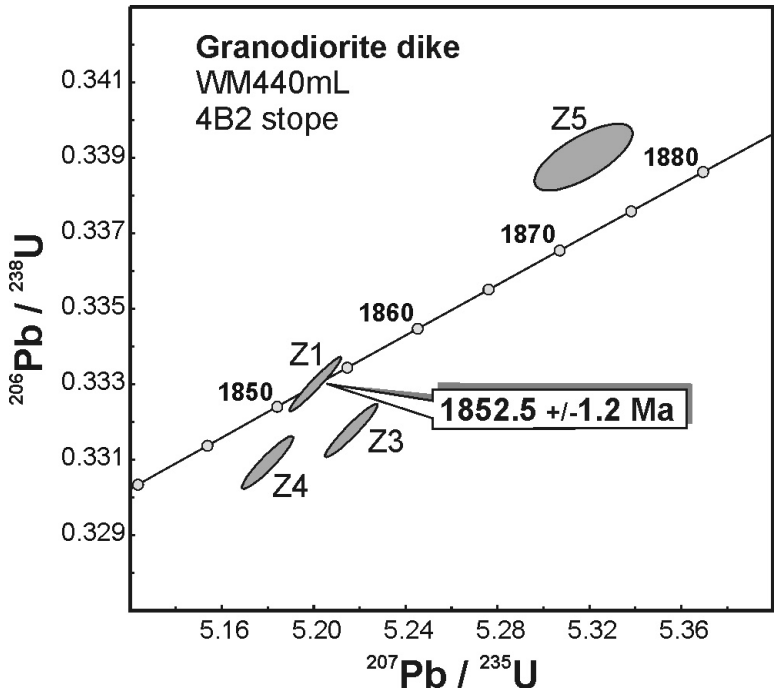

Figure 6: *Concordia diagram of U-Pb zircon analyses from the granodiorite dike on level WM440mL, 4B2 stope, Ruttan deposit. Data-point error ellipses are at the 95% confidence level.*

scale in the Rusty Lake belt by Baldwin (1988). As suggested by Speakman et al. (1982), the apparently higher grade of metamorphism in the mine area appears to result from contact metamorphism along the east margin of the Brehaut Lake pluton. The observed porphyroblast-matrix overprinting relationships constrain emplacement of this pluton to the late stages of the tectonothermal evolution of the mine area.

Sulphide mineralization

As mentioned previously, the spatial configuration and geometry of the sulphide lenses provides important, first-order insights into the macroscopic structure of the deposit and the MSU. In this section, these aspects of the principal sulphide lenses are described in detail, followed by general descriptions of the styles of mineralization and patterns of metal zoning, mineral textures and mesoscopic deformation structures, and sulphide remobilization effects. To the best of the authors' knowledge, this report provides the first comprehensive analysis of the configuration and geometry of the Ruttan deposit.

In order to facilitate description of the Ruttan deposit, the distribution of solid and near-solid sulphide has been compiled for two major levels in the Main and West mines, based on mapping by mine geologists (Figures 7, 8). These levels were selected because they are reasonably representative and divide the entire deposit into roughly equal thirds at similar elevations in both the Main and West mines (Figure 3). Representative vertical sections have also been compiled from drillhole sections of the mine (Figures 9–15). These sections, in contrast to the level plans, illustrate the probable ore outlines, which were delineated on the basis of a copper-equivalent assay cutoff (>1.0 wt.% Cu equivalent). In general, however, the probable ore outlines approximate the distribution of solid to near-solid sulphide, and the level plans and sections closely correspond. This point is illustrated by Figure 13, which shows the probable ore outlines for a portion of the Main mine, overlain by downhole histograms of iron content from drillhole assay data, which clearly indicate the distribution of solid and near-solid sulphide.

Macroscopic configuration and geometry

Traditionally, the principal sulphide lenses in the deposit have been designated with letters of the alphabet. In this contribution, these lenses are separated into three groups, based on their spatial distribution and structural setting (Figures 2, 3, 7 and 8): the B lenses, the West lenses (C, D, E, F) and the East lenses (H, J, K, L, JH, JN, JS). Art's Shear Zone (ASZ) separates the B lenses in the footwall from the West lenses in the hangingwall, whereas the East Shear Zone (ESZ) separates the West lenses in the footwall from the East lenses in the hangingwall. Traditionally, the B lens in the West mine was referred to as the 'West anomaly', and the B lens in the Main mine was grouped with the West lenses. In this report, however, these lenses are grouped together as the B lenses in order to emphasize their shared structural position in the footwall of the ASZ, as well as their distinctive mineralogical attributes (e.g., Ames and Taylor, 1996). As described in detail below and presented schematically in Figure 16, the D_2 and D_3 deformations are clearly manifested in the macroscopic distribution and geometry of the principal sulphide lenses: the B lenses are disposed in a train of lenticular, steeply plunging ore shoots along the trace of the D_3 North Wall Shear Zone (NWSZ), whereas the East and West lenses define a macroscopic isoclinal fold that is transected and displaced by D_3 shear zones, and is attributed to D_2 deformation.

B lenses

In the West mine, the B lens has a strike length of 350–400 m and is typically 10–15 m thick (Figures 7, 8). This lens is not exposed at surface and extends down dip from 170 to 1040 m below surface, with a general plunge of 55–65° to the southeast (Figure 3). On WM590mL, the B lens is offset by a narrow shear zone that dips to the south-southeast and displaces the hangingwall portion of the lens downward and to the west relative to the footwall (i.e., dextral-normal oblique slip; Figure 9). The thickness of the B lens in the West mine locally varies from less than 5 to 40 m over very short distances along strike and down dip. The thickest sulphide intervals typically coincide with portions of the lens that deviate in a northerly direction from the general east-northeast trend of the lens, and these intervals define copper-rich ore shoots that plunge 55–60° to the southeast, subparallel to the general plunge of the lens. As is evident near the eastern limit of the B lens on WM380mL, the macroscopic geometry of these intervals is suggestive of layer segments that have been back rotated in a kinematic regime of dextral strike-slip shear, with a minor component of normal oblique slip (Figure 7, inset). This kinematic regime is compatible with that indicated by asymmetric fabrics in the adjacent NWSZ.

In the Main mine, the B lens is laterally continuous at surface (Figure 2), with a strike length of about 500 m and a steep dip to the south-southeast. The lens is typically 10–15 m thick, but locally varies from less than 5 to 60 m over very short distances across strike and down dip. In the down-dip direction, the B lens separates into a series of discrete, regularly spaced, copper-rich ore shoots that plunge steeply to the southeast and exhibit progressively decreasing strike length and thickness with depth (Figure 3). The ore shoots extend to progressively deeper levels toward the eastern portion of the lens, with the deepest ore shoot ultimately pinching out 370 m below surface (Figure 3). Within the ore shoots, zones of zinc-rich mineralization and large diabase boudins trend at a slight counter-clockwise angle to the strike of the lens (Speakman et al., 1982). Unfortunately, the authors were unable to directly examine these features, as the B lens in the Main mine is almost completely mined out. Nevertheless, by analogy with the B lens in the West mine, it is hypothesized that the oblique orientation of the mineralization might result from back rotation, perhaps as a consequence of a shear differential between the NWSZ and ASZ.

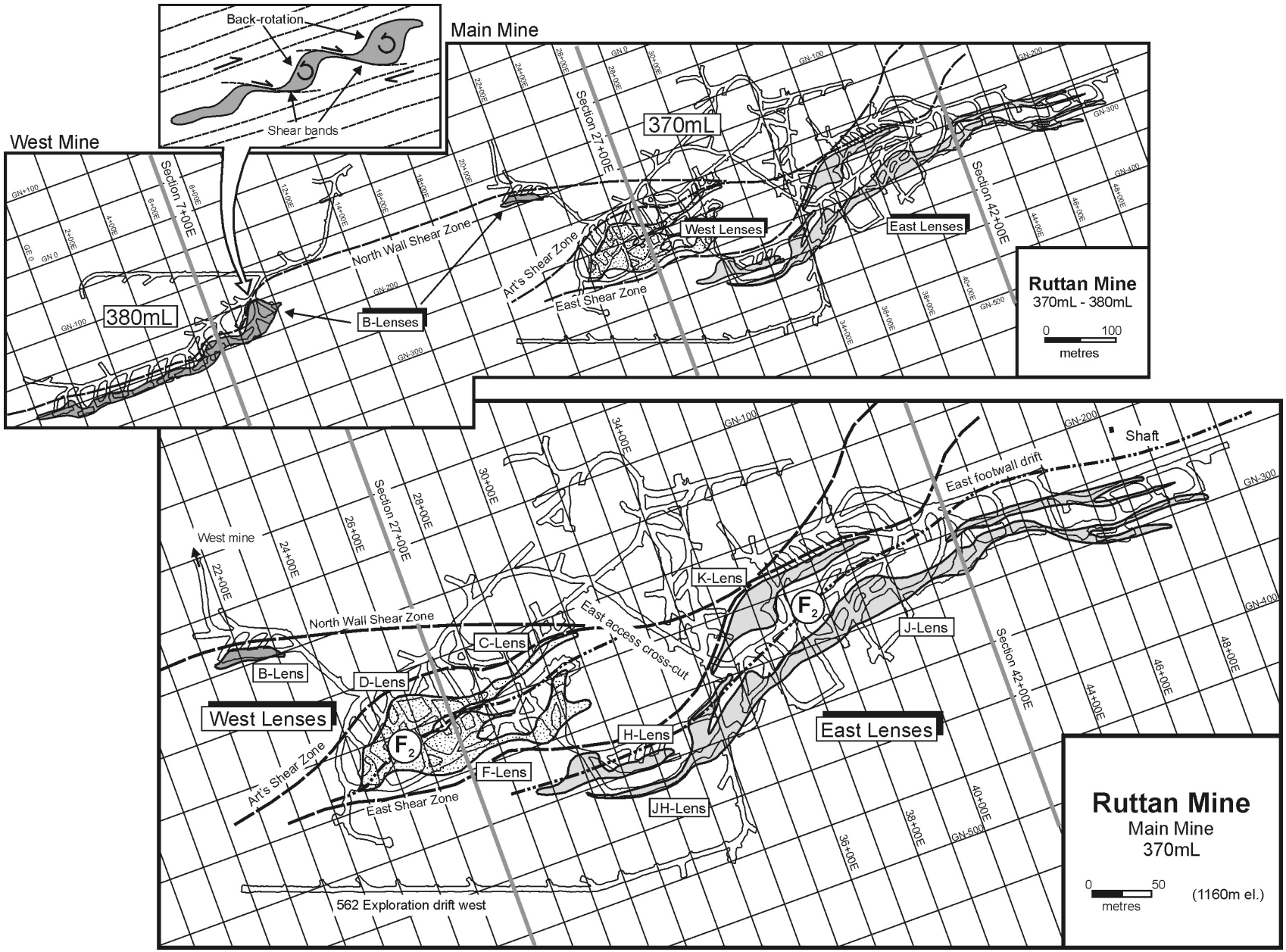

Figure 7: *Compilation level plan of MM370mL-WM380mL (top), Ruttan deposit, showing the distribution of solid and near-solid sulphide as mapped by mine geologists. The fill patterns correspond to those in Figure 2. The locations of sections 7+00E (Figure 9), 27+00E (Figure 10) and 42+00E (Figure 11) are indicated for reference by the heavy grey lines. The detailed plan of MM370mL (bottom) shows the principal sulphide lenses and macroscopic structural features. The inset (top left) illustrates a train of back-rotated layer segments, for comparison with the eastern portion of the B lens in the West mine (see text for discussion).*

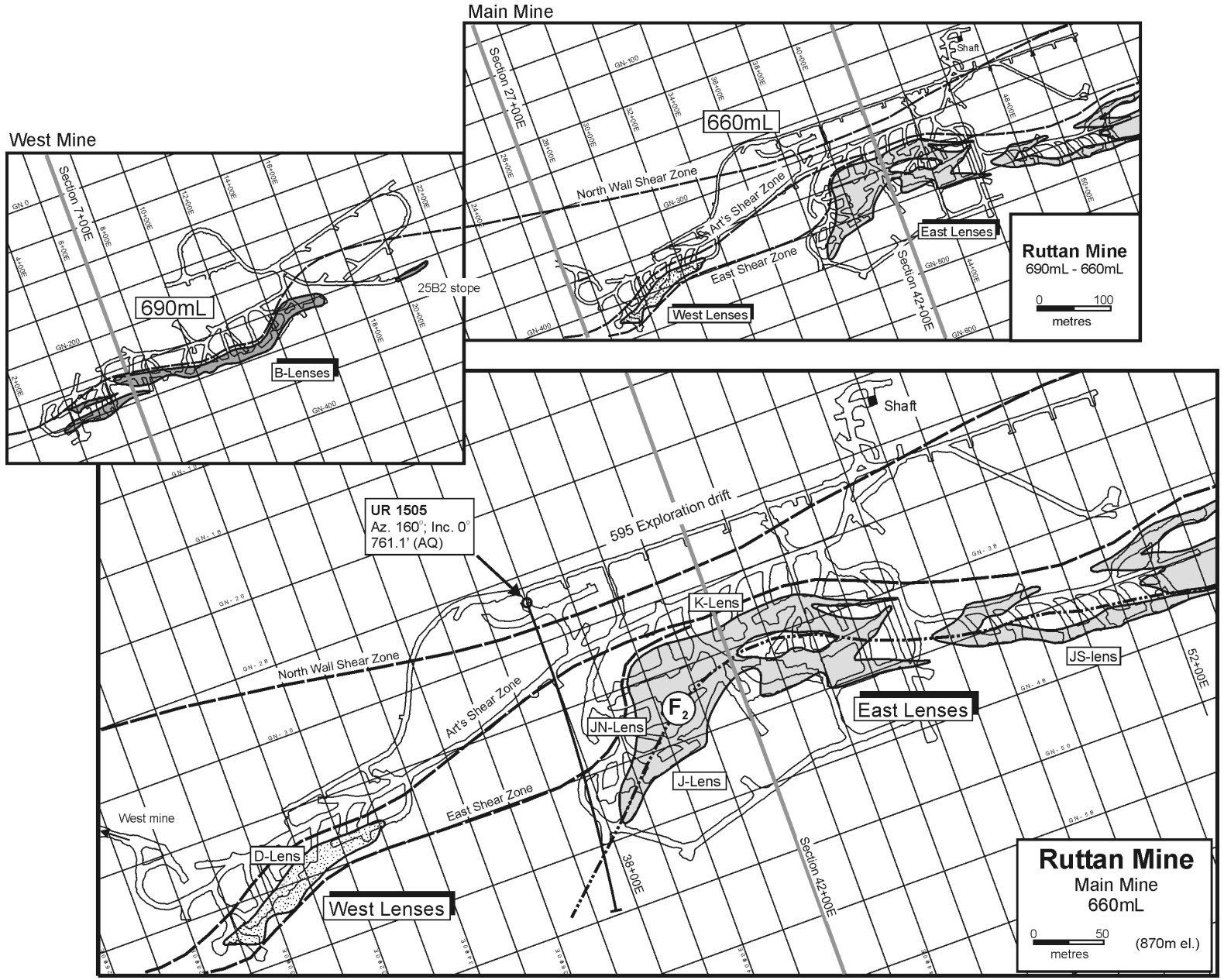

Figure 8: *Compilation level plan of MM660mL–WM690mL (top), Ruttan deposit, showing the distribution of solid to near-solid sulphide as mapped by mine geologists. The fill patterns correspond to those in Figure 2. The locations of sections 7+00E (Figure 9), 27+00E (Figure 10) and 42+00E (Figure 11) are indicated for reference by the heavy grey lines. Detailed plan of MM660mL (bottom) shows the principal sulphide lenses and macroscopic structural features. Note the location of drillhole UR1505, mentioned in the text.*

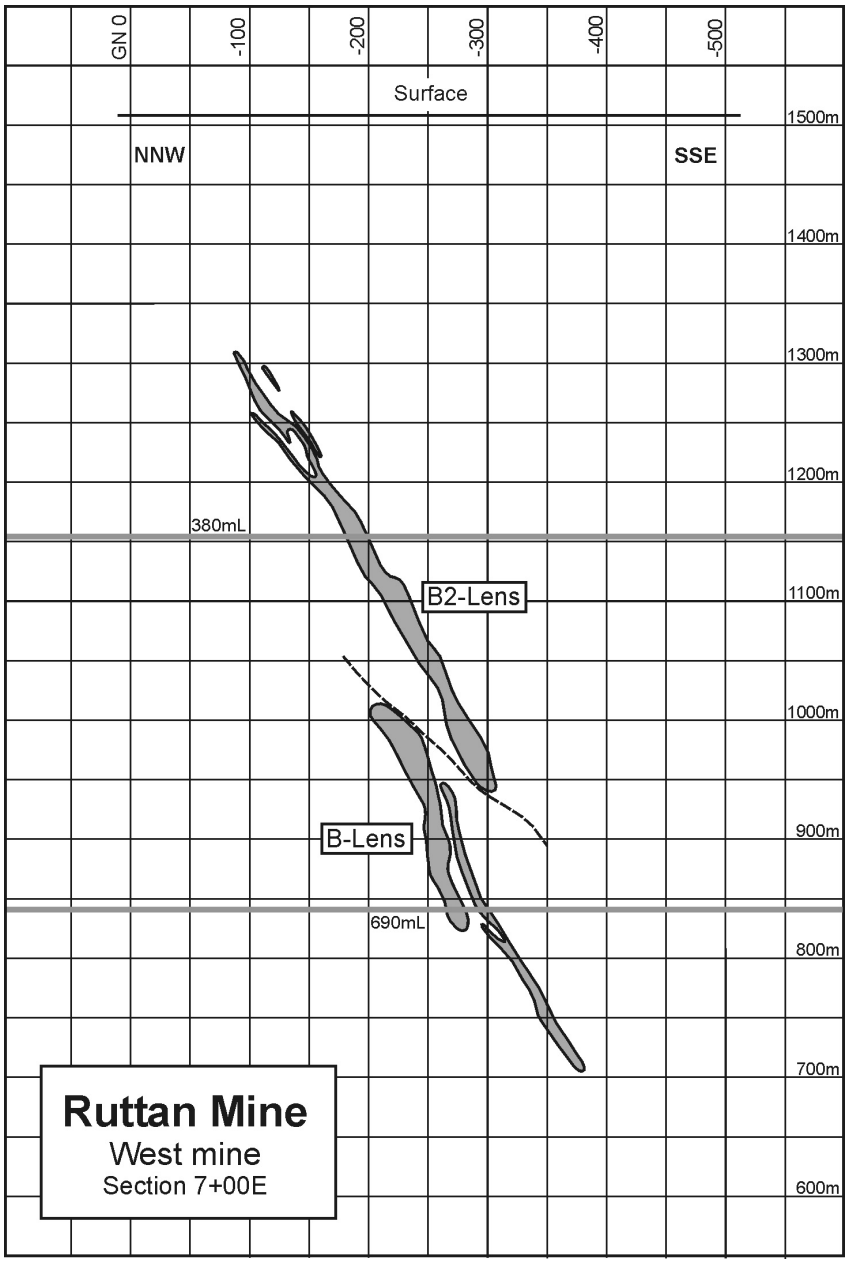

Figure 9: *Section 7+00E (looking east-northeast), Ruttan deposit, showing the distribution of probable ore (*see *text for discussion). The locations of WM380mL and WM690mL are indicated by the heavy grey lines. Dashed line indicates the location of the late shear zone that truncates the B lens on WM590mL (*see *text for discussion).*

West lenses

The West lenses group, which comprises the C, D, E and F lenses, constitutes a complex orebody that is bounded by the ASZ in the footwall and the ESZ in the hangingwall (Figure 2). At surface, the West lenses have a maximum strike length of approximately 350 m and contain intervals of solid sulphide that range up to 75 m thick. The thickest intervals are situated along the western termination of the West lenses and define a prominent copper-rich ore shoot that plunges 55–65° to the southeast, subparallel to the general plunge of the group. The strike length and thickness of this ore shoot gradually decrease down plunge. Below 550mL, this ore shoot forms a discrete, lenticular orebody that is tightly bounded between the ASZ and the ESZ (Figure 8) and pinches out 770 m below surface. Level plans above 400mL indicate that the West lenses are arranged in a tight, U-shaped map pattern (Figure 7), with a broad closure to the west defined by the thick ore shoot (D lens), and two thin apophyses that extend to the east, away from the closure, and are defined by the C lens in the footwall and the F lens in the hangingwall. On section 27+00E (Figure 10), the principal lenses clearly display a symmetric distribution about the D lens. This, in conjunction with the U-shaped map pattern and coincident extreme thickness of sulphide, is strongly suggestive of a macroscopic fold hinge. Unfortunately, the West lenses were completely inaccessible to direct examination underground, and relogging of several drillholes by the first author (UR253, UR337, UR462, UR1641) failed to provide unequivocal evidence of a major fold hinge.

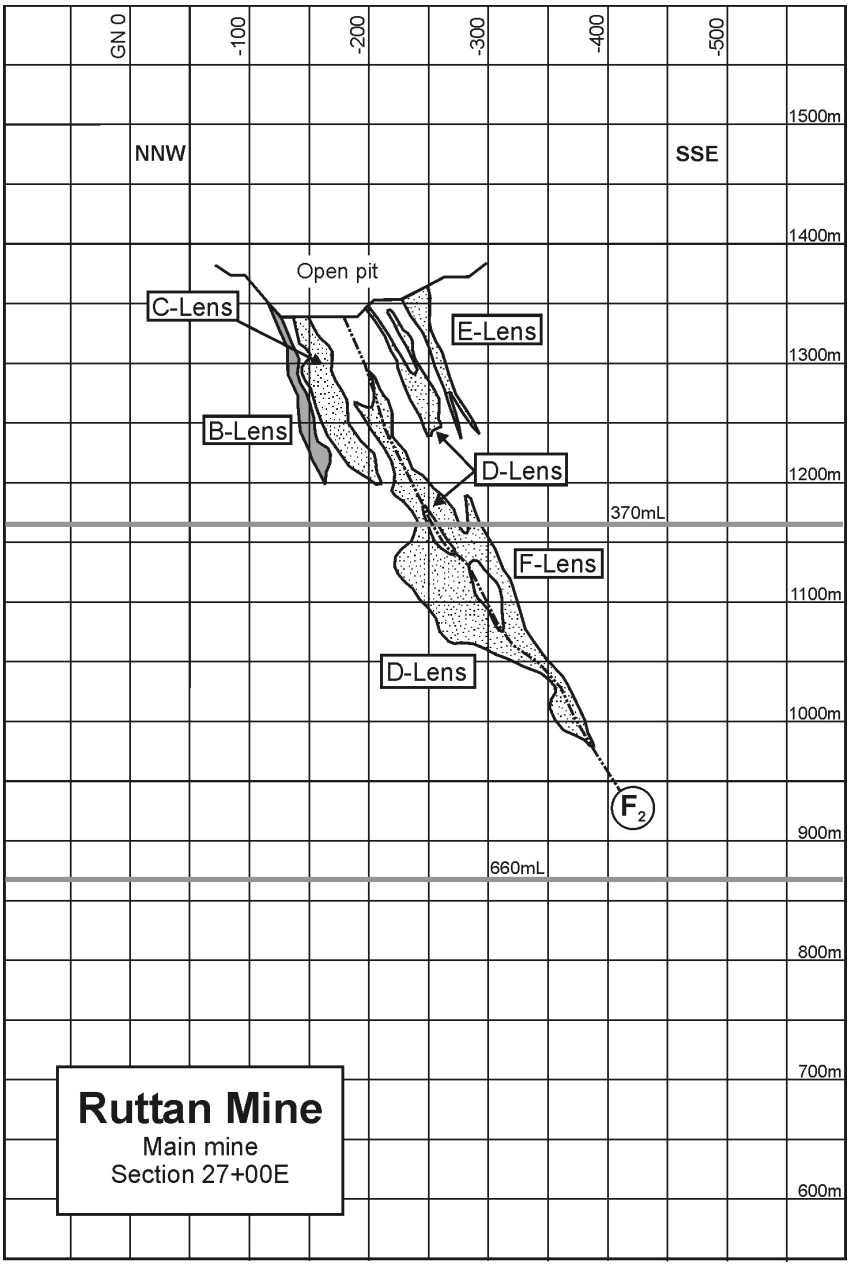

Figure 10: *Section 27+00E (looking east-northeast), Ruttan deposit, showing the distribution of probable ore. The locations of MM370mL and MM660mL are indicated by the heavy grey lines. Note the symmetric distribution of the principal sulphide lenses about an inferred macroscopic F_2 fold hinge (*see *text for discussion).*

Nevertheless, given the geometric similarity to the East lenses (*see* below), the authors believe that a fold model best explains the macroscopic geometry of the West lenses (Figure 16).

East lenses

The East lenses group, which consists mainly of the H, J, K, L, JH, JL and JS lenses, has a strike length of about 600 m and dips steeply to moderately to the south-southeast. These lenses extend down dip from surface for more than 1000 m with a general plunge of 55–60° to the southeast, and remain open to the east along strike and down plunge to the southeast (Figure 3). Level plans above 800mL (Figures 7, 8) indicate that the East lenses are arranged in a tight, roughly U-shaped map pattern analogous to that of the West lenses. This structural geometry is particularly evident in mine-scale sections through the medial portion of the East lenses (Figures 11, 12). On these sections, the distribution of solid to near-solid sulphide in the MSU defines a macroscopic isoclinal synform that is overturned to the north-northwest, with a relatively intact hangingwall limb defined by the main J lens and a strongly attenuated footwall limb defined by the K and L lenses. In the fold hinge, the J and K lenses merge (Figure 13) to form a major, copper-rich ore shoot that plunges 55° to the southeast along the western termination of the East lenses (Figure 3). Below 800mL, the fold-hinge ore shoot ranges up to 90 m in thickness within a strike length of less than 300 m, and thus forms a remarkable cylindrical orebody that plunges 45° to the east and abruptly

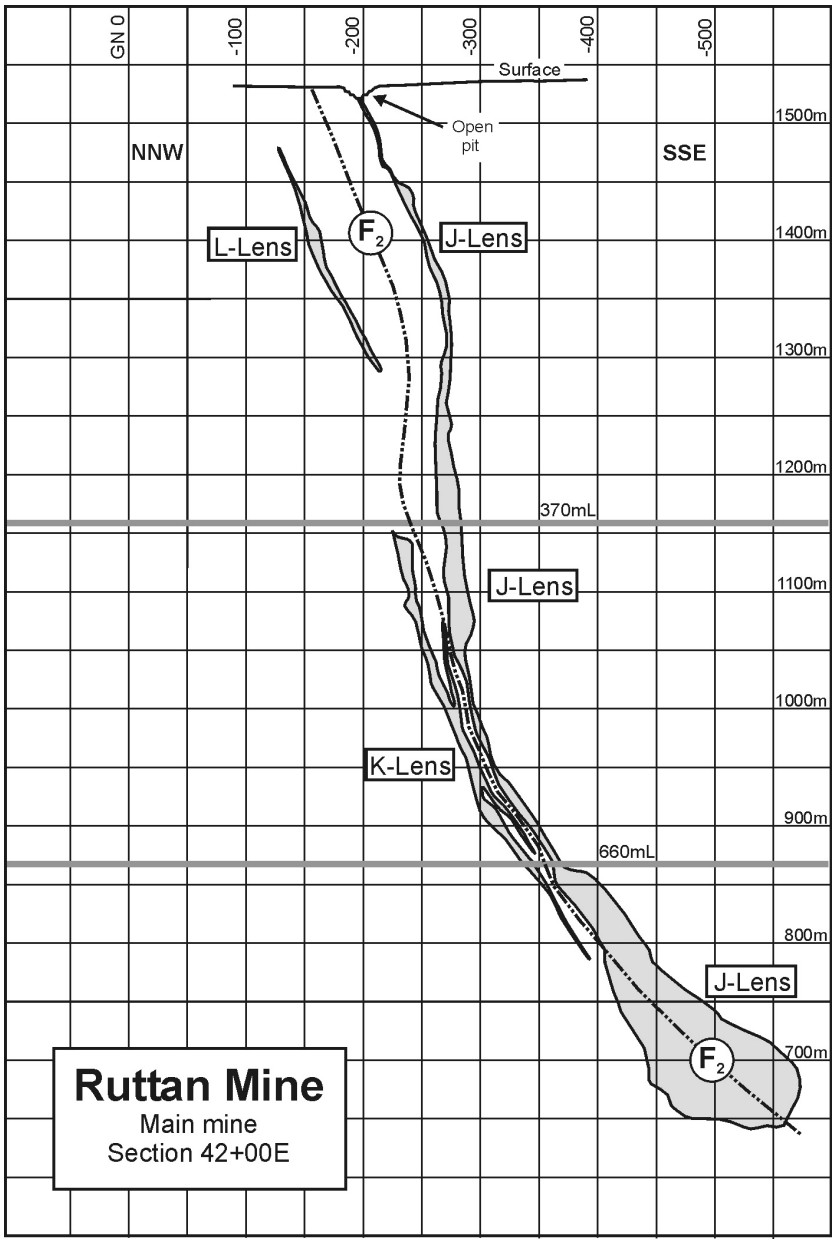

Figure 11: *Section 42+00E (looking east-northeast), Ruttan deposit, showing the distribution of probable ore. The locations of MM370mL and MM660mL are indicated by the heavy grey lines. Note the symmetric distribution of the principal sulphide lenses about the macroscopic F_2 fold hinge.*

pinches out 50 m below 1000mL (Figure 3). Along strike 275 m to the east, the JS lens also clearly delineates the fold hinge (Figures 14 and 15) and forms a major ore shoot that plunges 40–45° to the east (Figure 3). Drillhole UR1505, which was drilled subhorizontally from footwall to hangingwall on MM660mL (Figures 8 and 13), cuts the axial plane of the fold immediately west of the fold-hinge ore shoot. Fabric relationships observed in core from this hole confirm the presence of the fold (Figure 17).

Style of mineralization and patterns of metal zoning

Sulphide mineralization in the Ruttan deposit is principally composed of pyrite, with highly variable, though generally subordinate, proportions of pyrrhotite, chalcopyrite and sphalerite, and very minor galena. Common gangue minerals include chlorite, biotite, quartz, anthophyllite, magnetite, talc, anhydrite, gypsum, calcite and gahnite, in order of decreasing general abundance. On the basis of sulphide mineral assemblage and general style of mineralization, three principal types of sulphide mineralization are distinguished in the deposit. In this report, these are referred to as copper-rich massive sulphide, zinc-rich layered sulphide and copper-rich stringer sulphide (*see also* Ames and Taylor, 1996). The copper-rich massive and zinc-rich layered sulphide form the most significant orebodies in the deposit, and the distribution of these ores is clearly reflected in bulk-scale patterns of metal zoning (e.g., Barrie and Taylor, 2001, Figure 7).

Copper-rich massive sulphide is the most common type of ore in the Ruttan deposit. This ore consists mainly of

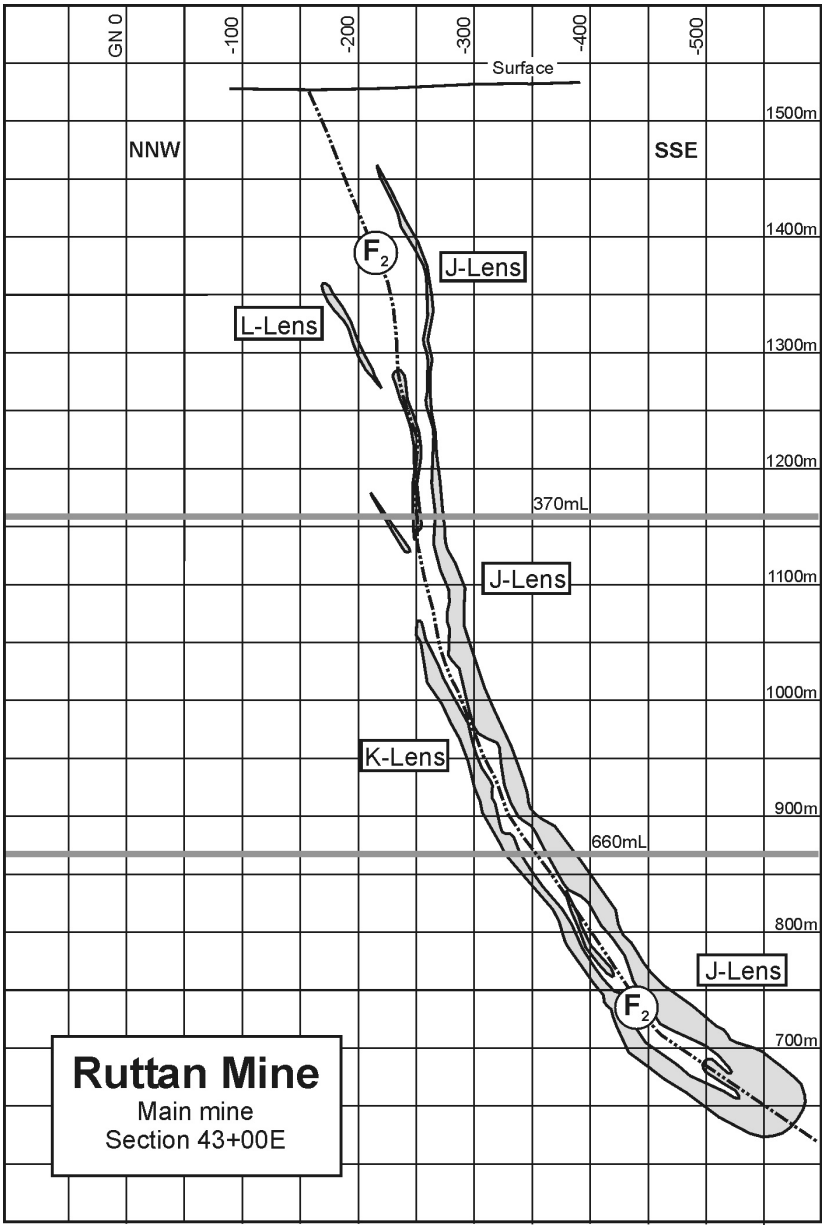

Figure 12: *Section 43+00E (looking east-northeast), Ruttan deposit, showing the distribution of probable ore. The locations of MM370mL and MM660mL are indicated by the heavy grey lines. Note the symmetric distribution of the principal sulphide lenses about the macroscopic F_2 fold hinge.*

medium-grained equigranular pyrite, typically with subordinate pyrrhotite (>2:1 pyrite:pyrrhotite), chalcopyrite (<6%) and sphalerite (<1%). The massive ore contains 60–95% total sulphide and ranges from remarkably homogeneous solid sulphide to near-solid sulphide that contains up to 40% silicate minerals and wallrock inclusions (Figure 5d). The massive ore ranges up to 90 m in thickness in the major ore shoots that define the western limits of both the East and West lenses. This ore is laterally extensive in the basal portions of the B lenses, although, in these locations, it contains a greater proportion of pyrrhotite (typically 30%, but locally up to 80%) and up to 20% magnetite (Ames and Taylor, 1996), which is a distinguishing characteristic of the B lenses (Speakman et al., 1982).

The zinc-rich layered sulphide contains 60–90% total sulphide and comprises rhythmically alternating layers of solid to near-solid, pyrite-rich or sphalerite-rich sulphide that range from 1 to 10 cm thick (Figure 5e). The layered ore typically consists mainly of pyrite, with subordinate sphalerite (5–15%), pyrrhotite (<10%) and chalcopyrite (<2%). Layered sulphide forms laterally extensive zones up to 10 m thick in the eastern portion of the East lenses, particularly in the hangingwall of the J and JS lenses (i.e., the 'sedimentary sulphide lens' of Speakman et al., 1982), and is also locally present in the hangingwall of the B lens, although it is not laterally extensive (Ames and Taylor, 1996).

Copper-rich stringer sulphide is particularly well developed in the immediate footwall of the B lens in the West mine, where Ames and Taylor (1996) described rhyolite- and chlorite-schist–hosted stringer sulphide defined by a variably transposed network of pyrrhotite-pyrite-chalcopyrite veins that range from

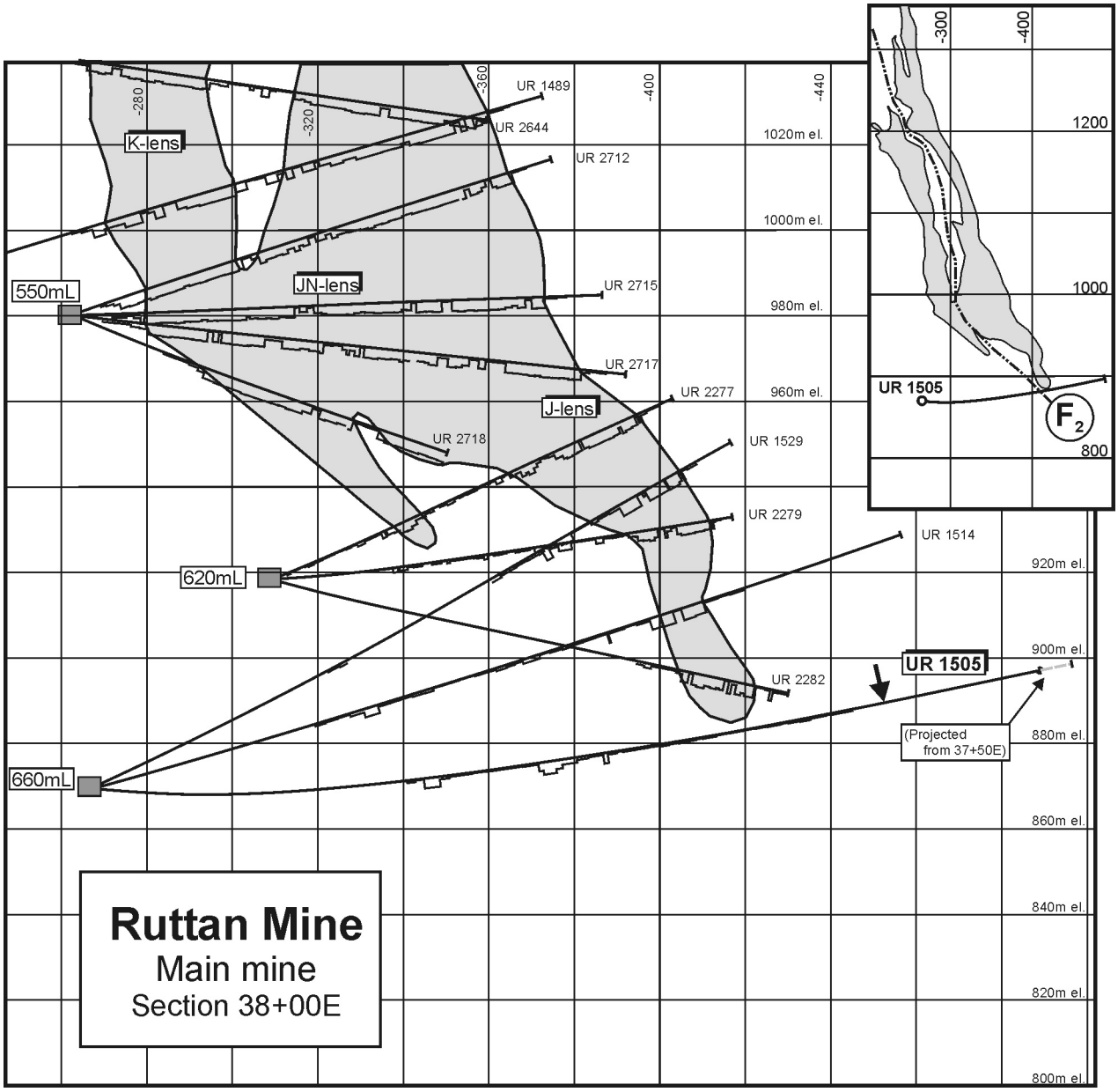

Figure 13: *Section 38+00E (looking east-northeast), Ruttan deposit, showing the distribution of probable ore at the western limit of the East lenses between MM490mL and MM660mL. Definition drillholes are indicated, and include downhole histograms of Fe content (*see *text for discussion). Inset (top right) shows the macroscopic geometry of the East lenses, and the axial trace of the macroscopic F_2 fold. Note the location of drillhole UR1505, mentioned in the text (heavy arrow indicates the location of the fold hinge in drillcore). The apparent offset between the axial trace of the F_2 fold (inset) and the fold hinge observed in drillhole UR1505 is a projection effect (*see *Figure 8).*

0.5 to 30 cm thick. These veins typically account for 20–40% of the stringer sulphide zone and locally grade continuously upward into copper-rich massive sulphide in the basal portion of the B lens. As proposed by Ames and Taylor (1996), this stringer-style mineralization appears to represent a strongly transposed syngenetic feeder system in the footwall of the B lens. In the Main mine, however, the situation is less clear and the authors are aware of only one clear example of copper-rich stringer sulphide, which is hosted by strongly sericitized felsic volcanic rocks in the immediate footwall of the JS lens in the East lenses (MM800mL, 37J1 stope). In this location, pyrrhotite-chalcopyrite-pyrite veinlets up to 2 cm thick locally constitute up to 50% of the footwall and define a distinct, generally concordant zone of irregular stockwork veins (Figure 5f) that ranges up to 1.5 m thick. This zone grades continuously upward into copper-rich massive ore, which in turn grades upward into zinc-rich layered ore. Similar gradations are locally observed in the B lens in the West mine, and suggest that these particular lenses are stratigraphically upright. The significance of these data is addressed in the 'Discussion' section.

In the late stages of mining, a new style of ore was discovered in one location on level MM265mL and was briefly examined by the authors in the 40J-HW ('HW zinc') stope

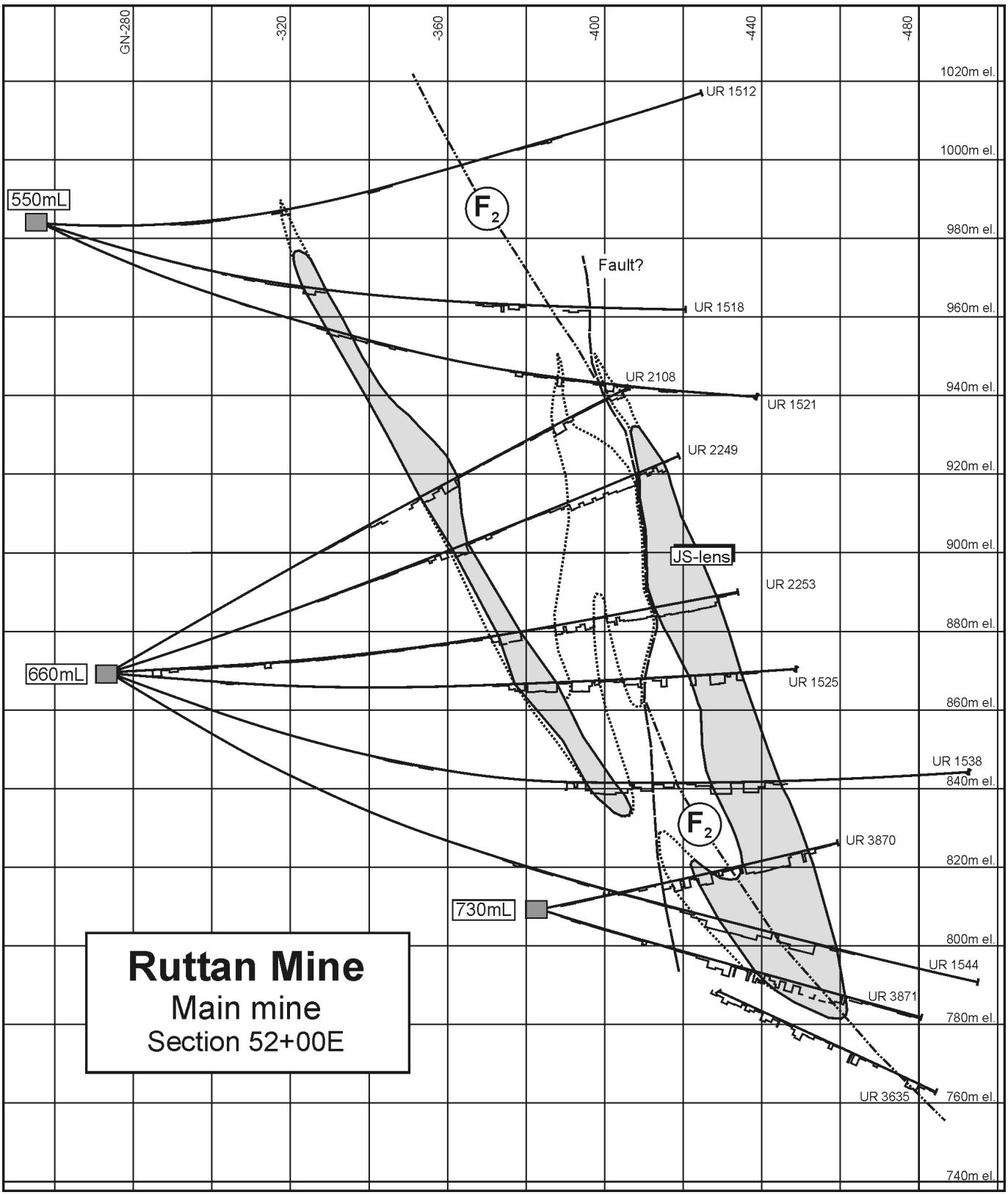

Figure 14: *Section 52+00E (looking east-northeast), Ruttan deposit, showing the distribution of probable ore near the eastern limit of the East lenses between MM550mL and MM800mL. Definition drillholes are indicated and include downhole histograms of Fe content. The dotted lines indicate the outline of solid to near-solid sulphide that apparently did not constitute probable ore in the 2002 ore model. Note the location of the macroscopic F_2 fold hinge.*

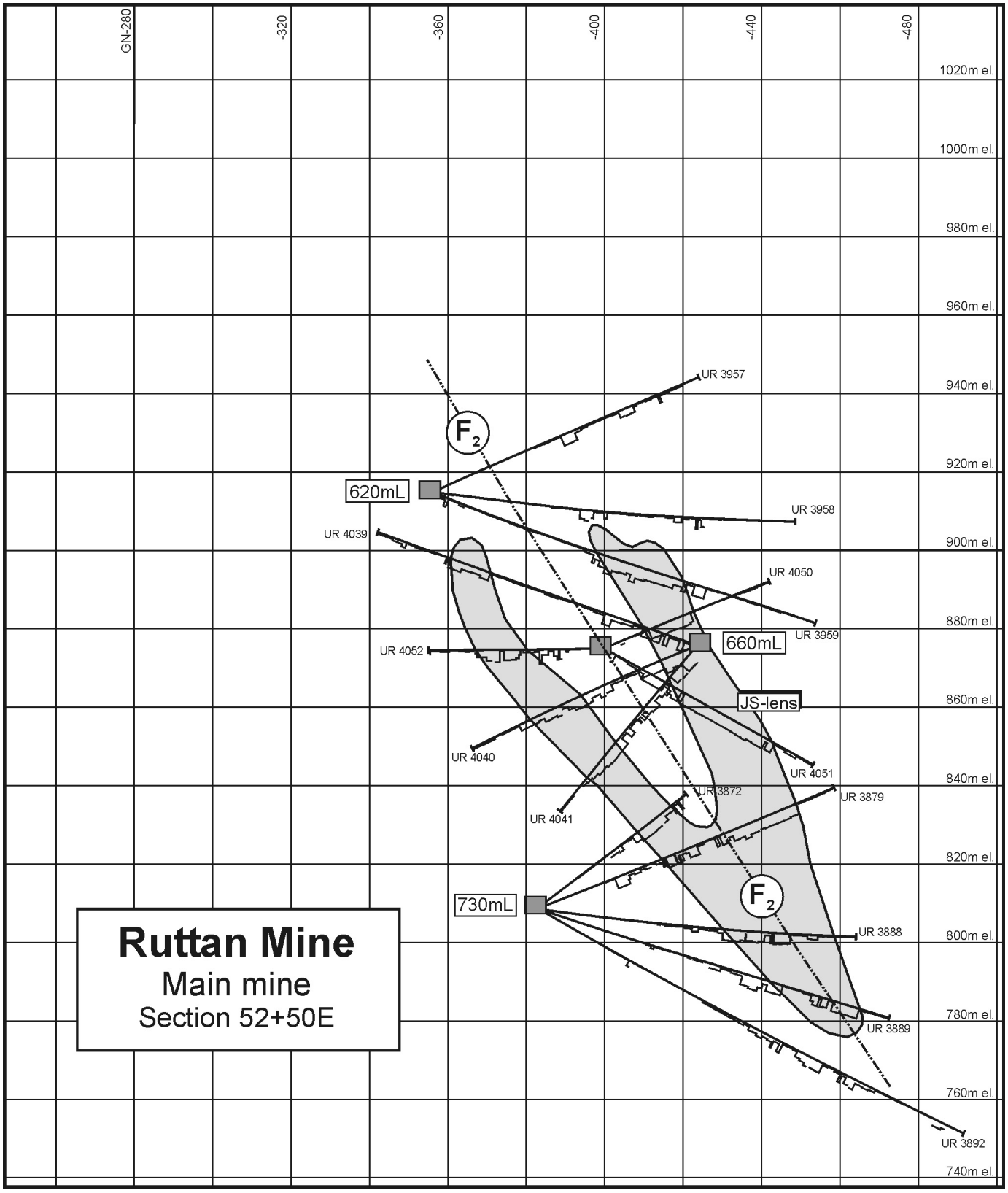

Figure 15: *Section 52+50E (looking east-northeast), Ruttan deposit, showing the distribution of probable ore near the eastern limit of the East lenses between MM620mL and MM800mL. Definition drillholes are indicated, and include downhole histograms of Fe content. In this location, the outline of probable ore clearly defines the macroscopic F_2 fold hinge.*

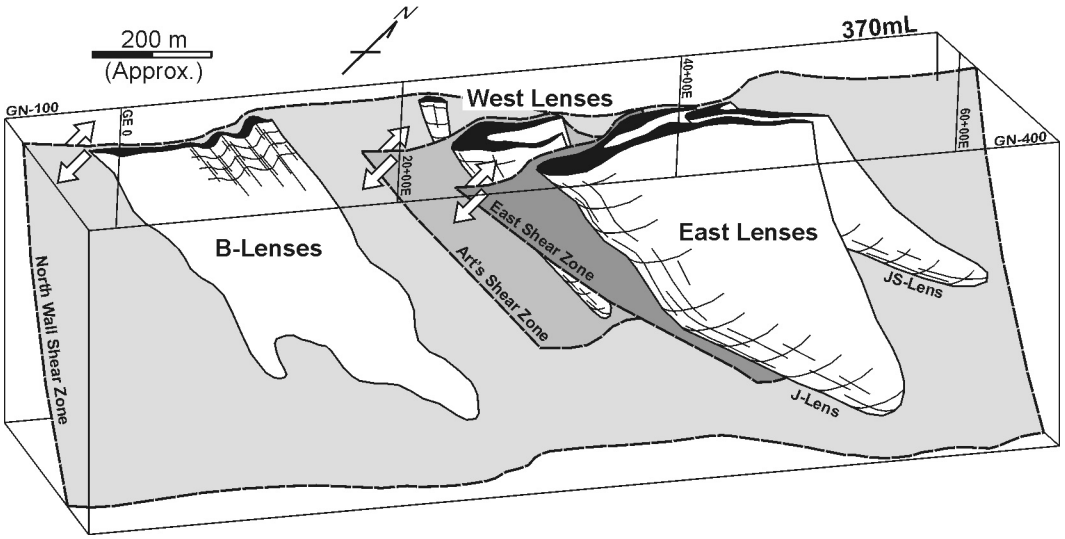

Figure 16: *Schematic structural model of the Ruttan deposit, illustrating the configuration and geometry of the principal sulphide lenses with respect to the major structural features identified in the West and Main mines (see text for discussion). Note that the eastern limit of the East lenses is an economic cutoff; these zinc-rich lenses extend for significant distances along strike to the east of the 2002 ore model.*

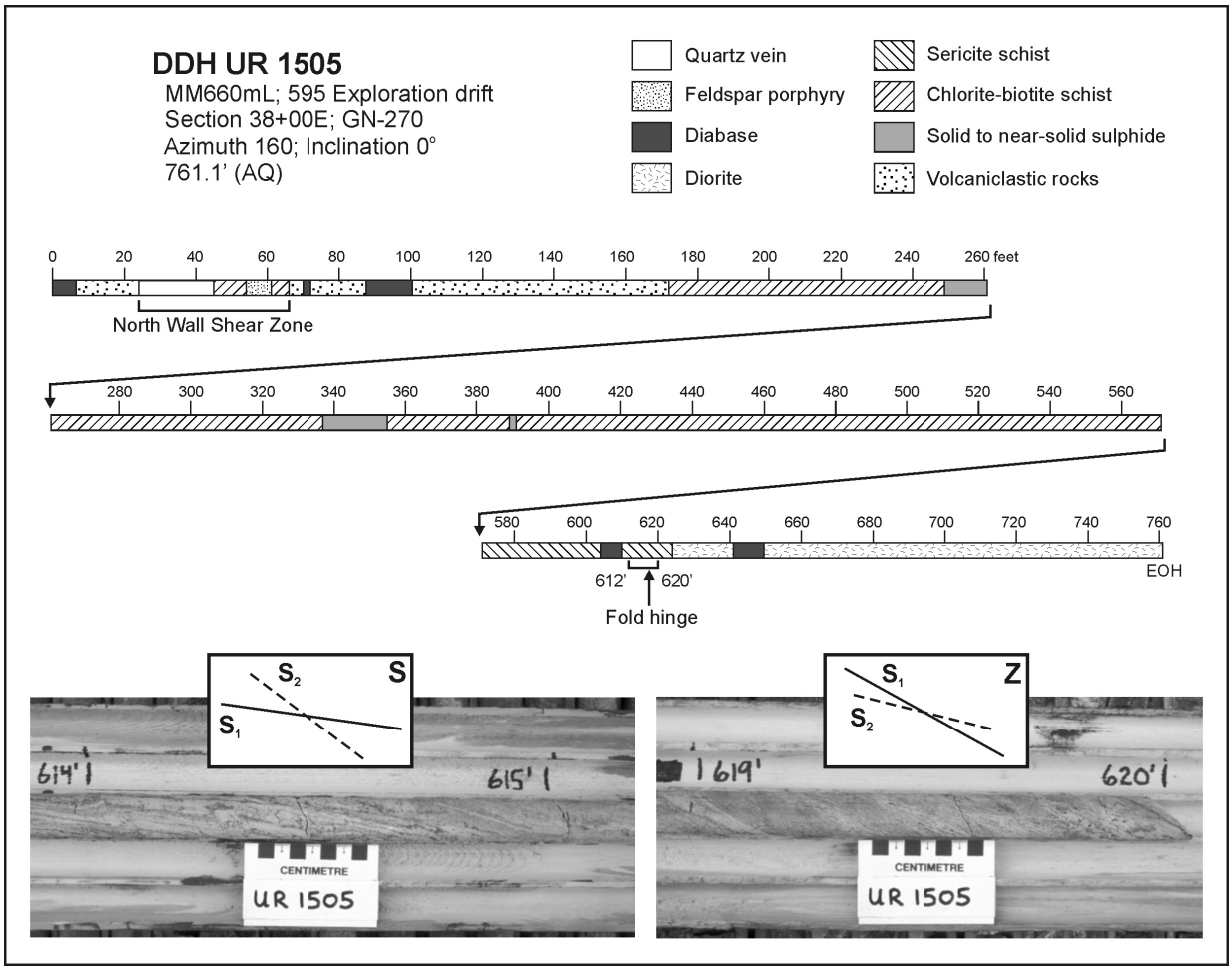

Figure 17: *Diagrammatic log of drillhole UR1505, Ruttan deposit. The F_2 hinge is observed in an intact section of drillcore between 612 and 620 feet downhole. This section of drillcore is complete (no lost or ground core), and none of the broken segments was rotated in the core barrel during drilling. The photographs illustrate the change in vergence (S_1-S_2) on opposite limbs of the fold. Note that the layering (S_1) is nearly parallel to the drillcore axis at 614', and that the southern limb of the fold is cut by the Corner Lake diorite pluton (*see also *Figure 2).*

(Figure 3), which is developed 100 m into the hangingwall of the East lenses on a small, irregular body of high-grade zinc ore that is hosted by epidotized biotite schist of the Powder Magazine unit. In this stope, the ore is invaded by a swarm of fine-grained diabase dikes and comprises homogeneous solid sulphide (>90% total sulphide) that consists mainly of coarse-grained, equigranular sphalerite (>90%), with less than 10% combined pyrrhotite, galena, pyrite and chalcopyrite, in order of decreasing relative abundance. The zinc and silver contents of this ore are generally an order of magnitude higher than those of the Ruttan deposit, and the lead content is two orders of magnitude higher (R. Yaworski, pers. comm., 2002). Hence, the character and setting of the HW zinc orebody are significantly different from the main Ruttan deposit, perhaps indicating a distinct genesis. This orebody is not discussed further in this report.

Mineral textures and mesoscopic deformation structures

Sulphide mineral textures in the Ruttan deposit typically record intense annealing recrystallization. Pyrite, pyrrhotite and sphalerite are coarsely crystalline and commonly exhibit granoblastic textures, particularly in solid sulphide. Pyrite also commonly forms idioblastic porphyroblasts up to 5 cm across that, in near-solid sulphide, contain abundant inclusions of accessory silicate phases. Chalcopyrite tends to form irregular blebs along the margins of coarser sulphide grains, or fine-scale piercement veinlets that crosscut granoblastic aggregates of sulphide minerals. Large porphyroblasts of pyrite often exhibit evidence of brittle failure, and the resulting fracture networks are filled with stockwork veinlets of chalcopyrite. Similar relationships are observed on a larger scale in brittle fracture networks in crosscutting diabase dikes (Figure 18a). Domains of low finite strain, such as boudin necks and fold hinges, also contain blebs and veinlets of chalcopyrite, typically in association with vein quartz and anhydrite (Figure 18b). These features indicate fluid-state remobilization of chalcopyrite.

Although solid sulphide tends to be strongly annealed, a weak planar fabric is locally evident and is defined by a preferred alignment of accessory silicate phases (principally biotite and anthophyllite). Varying proportions of granoblastic sulphide minerals in these rocks locally define a diffuse, centimetre-scale gneissic layering that parallels the planar fabric. As the proportion of accessory silicate phases increases, the planar fabric becomes more prominent and near-solid sulphide typically contains a pervasive planar fabric, defined by a preferred alignment of biotite, chlorite, anthophyllite and elongate sulphide minerals (mainly pyrite). This fabric locally forms a penetrative schistosity (Figure 18c), and the resulting rocks are properly described as near-solid sulphide schist or tectonite (e.g., Park, 1996). In several locations, elongate biotite and pyrite grains also define a penetrative linear fabric in the sulphide schist, which thus constitutes L-S tectonite.

The near-solid sulphide schist is typically developed along the margins of solid-sulphide mineralization and forms laterally continuous zones that range up to 15 m thick. Speakman et al. (1982) described lenticular zones of near-solid sulphide schist in the central portions of the ESZ and ASZ. Typically, the schist contains very well developed shear-sense indicators, including S-C fabrics, shear bands (Figure 18c), foliation fish and back-rotated layer segments, that indicate high finite strain and a noncoaxial deformation path. In all cases, these asymmetric fabrics indicate dextral shear, with a variable component of normal oblique slip. A prominent tectonite layering, locally developed in these zones, is defined by interleaved, lenticular layers of solid sulphide, near-solid sulphide schist and silicate schist that range up to 50 cm thick. Abundant, tight to isoclinal, rootless and intrafolial fold closures provide evidence of progressive folding and transposition in these zones. These folds have highly attenuated limbs, and markedly thickened hinges that contain irregular veinlets and blebs of remobilized chalcopyrite. Layered near-solid sulphide schist in the 1B2FW stope (level WM440mL) records at least two cycles of folding and transposition (Figure 19a), as indicated by the presence of two early generations of intrafolial isoclinal folds, which are refolded by open, Z-asymmetric folds. In the footwall of the B lens in the West mine, thick zones of sulphide-silicate schist locally contain spectacular penetrative S-C fabrics (Figure 18d), with clear evidence of progressive folding, disruption and disaggregation of wispy folia of chlorite-biotite schist in a ductile matrix of chalcopyrite and pyrrhotite during noncoaxial deformation (i.e., *durchbewegung*; Marshall and Gilligan, 1989).

Boudin structures are evident on a variety of scales throughout the Ruttan deposit, but are most prevalent in the B lenses (Speakman et al., 1982; Ames and Taylor, 1996). In the West mine, foliated sulphide schist contains boudins of granodiorite up to 10 m across, which form prominent trains that parallel the trend of the lens (Ames and Taylor, 1996). The tectonite layering in the sulphide schist wraps around the boudins and is locally tightly folded into the boudin necks. Irregular pods and veins of quartz, chalcopyrite, pyrrhotite and anhydrite are typically present in the boudin necks and are relatively undeformed. In this regard, the boudin structures provide clear mesoscopic evidence of sulphide remobilization via both solid-state (i.e., ductile flow) and fluid-state processes.

Sulphide remobilization

Remobilization in the context of stratiform VMS deposits can be defined as the micro-, meso- and macroscopic translocation of pre-existing solid and near-solid sulphide, resulting in modified patterns of concentration or distribution (e.g., Gilligan and Marshall, 1987; Marshall and Gilligan, 1993). As described by Marshall and Gilligan (1993), remobilization of stratiform ore may involve 1) internal redistribution of sulphide, where the layer boundary integrity is largely maintained, or 2) external redistribution, where the layer boundary integrity has been substantially transgressed and there has been a significant departure from primary conformable relationships, with the possible formation of separate new orebodies. In either case, the remobilization can involve either chemical (liquid-state) or mechanical (solid-state) processes.

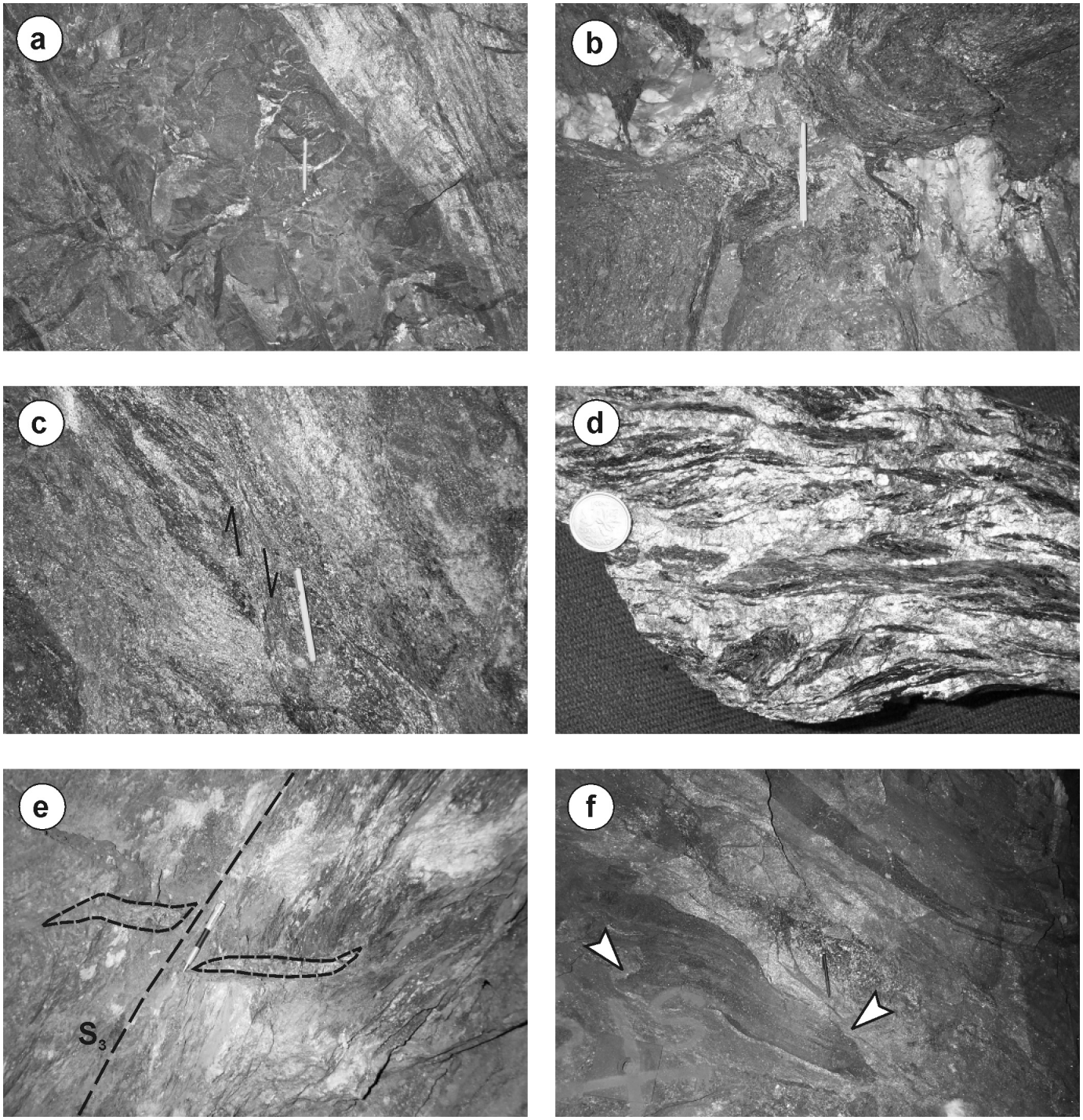

Figure 18: *Photographs of sulphide mineralization, Ruttan deposit:* ***a)*** *stockwork chalcopyrite veins hosted by brittle fracture networks in a late-kinematic diabase dike that crosscuts solid to near-solid sulphide schist near the footwall of the JS lens, wall exposure (facing east), level MM800mL, 37J1 stope (pencil for scale);* ***b)*** *chalcopyrite-filled boudin neck between segments of a boudinaged quartz vein in the footwall of the B lens, wall exposure (facing northeast), level WM280mL, 9B2 stope (pencil for scale);* ***c)*** *solid and near-solid sulphide schist in the footwall of the JS lens, wall exposure (facing east), level MM800mL, 37J1 stope; note well-developed shear band (marked by arrows) to the left of the pencil;* ***d)*** *grab sample of near-solid sulphide schist from the footwall of the B lens, showing prominent S-C fabrics, foliation fish and asymmetric folds defined by wispy folia of chlorite schist in a matrix of solid chalcopyrite and pyrrhotite, level WM950mL, ore pass (coin for scale);* ***e)*** *chalcopyrite-filled tension gashes (outlined) cutting chlorite schist and the S_3 foliation in the East Shear Zone, wall exposure (facing southwest), level MM370mL, east access crosscut (pencil for scale);* ***f)*** *solid sulphide schist containing foliated wallrock inclusions, wall exposure (facing northeast), level WM280mL, 9B2 stope; note the local angular discordance between the fabric in the solid sulphide and the inclusions (marked by arrows; pencil for scale).*

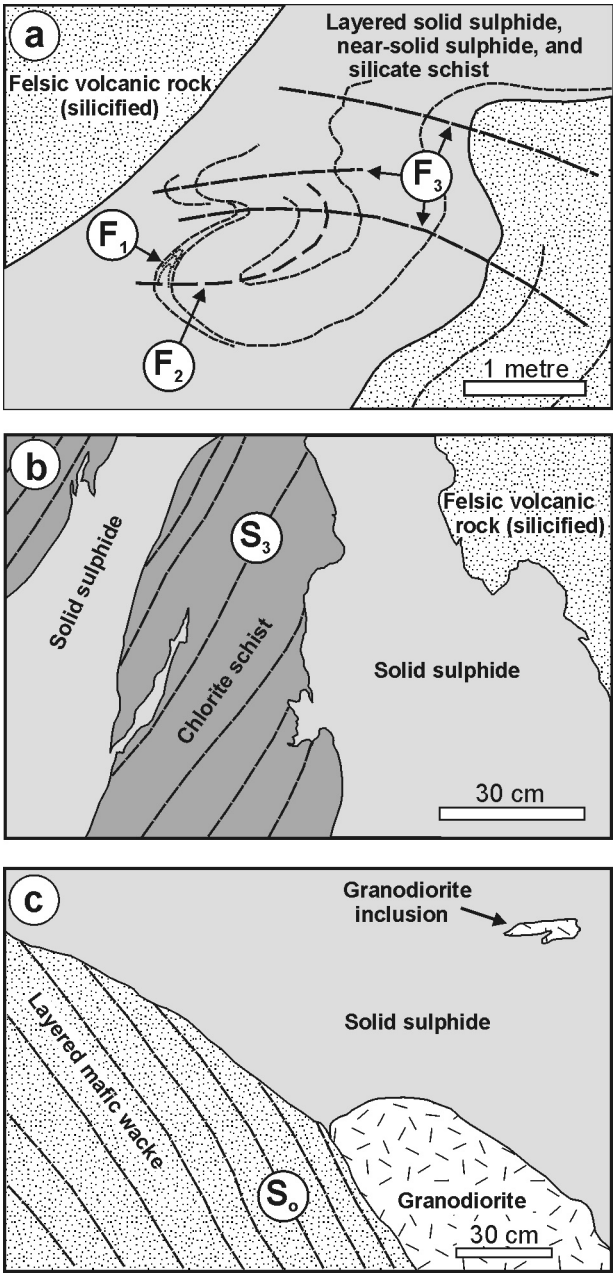

Figure 19: *Simplified sketches (from photographs) of observed structural overprinting and crosscutting relationships in solid and near-solid sulphide from the Ruttan deposit (*see *text for discussion):* ***a)*** *evidence of multiphase folding and transposition in layered sulphide schist in the footwall of the B lens, wall exposure (looking northwest), level WM440mL, 1B2FW stope;* ***b)*** *discordant veins of solid sulphide cutting chlorite schist and the S_3 foliation in the East Shear Zone, wall exposure (looking southwest), level MM370mL, east access crosscut;* ***c)*** *discordant body of solid sulphide cutting layered (S_o) mafic wacke and a granodiorite sill in the hangingwall of the B lens, wall exposure (looking northeast), level WM690mL, 25B2 stope.*

In the case of the Ruttan deposit, the mesoscopic mineral textures and deformation structures described in the preceding paragraphs provide clear evidence of internal remobilization of sulphide on a micro- to mesoscopic scale. This remobilization has obscured primary depositional features in solid and near-solid sulphide, and has significantly modified primary patterns of metal zoning and mineralization style within individual sulphide lenses (e.g., Figure 19a). Mesoscopic, tight to isoclinal folds in solid and near-solid sulphide are characterized by highly attenuated limbs and markedly thickened hinges, which are a natural consequence of folding a relatively incompetent sulphide layer within a layered package of relatively competent rocks under high-temperature metamorphic conditions (e.g., van Staal and Williams, 1984; Gilligan and Marshall, 1987). As described by Marshall and Gilligan (1993), internal remobilization of sulphide during folding can also produce significant variations in metal ratios between fold limbs and hinge, with the relatively mobile phases concentrated in the hinges and the relatively immobile phases concentrated in the limbs. In the case of the Ruttan deposit, evidence of this process is observed on a mesoscopic scale in the form of chalcopyrite mobilizate in F_2 fold hinges.

External remobilization of sulphide, in which primary layer-boundary constraints have been substantially transgressed, is most clearly indicated on a mesoscopic scale in the Ruttan deposit by vein-like bodies of solid sulphide that crosscut the S_3 foliation in the major D_3 shear zones. At the southeast end of the east access crosscut on level MM370mL (Figure 7), for example, the S_3 foliation in the ESZ is crosscut by subhorizontal tension gashes up to 20 cm thick that are filled with solid chalcopyrite (Figure 18e). Several vein-like bodies of homogeneous solid sulphide (pyrite) also cut the shear zone in this location (Figure 19b) and range up to 3 m thick. The contacts of the sulphide veins are irregular and wavy but remarkably sharp, and locally cut across the penetrative S_3 foliation in the chlorite schist at an orthogonal angle (Figure 19b). In these locations, there is no deflection of the S_3 foliation along the margins of the sulphide, and the strongly annealed sulphide contains no evidence of a planar fabric.

In the immediate hangingwall of the ESZ on level MM370mL, angular blocks of wallrock up to several metres across locally constitute up to 40% of the K lens and are randomly oriented in a homogeneous matrix of solid sulphide. This block-in-matrix texture is a common feature of the thick, copper-rich ore shoots in the Ruttan deposit (e.g., Speakman et al., 1982) and is developed on a variety of scales (Figures 5d, 18f). Spectacular examples of this texture in the 9B2 stope on level WM280mL and the 16B stope on level WM540mL comprise angular blocks of silicate schist and granodiorite, up to several metres across, supported in a matrix of coarse, recrystallized solid sulphide. The blocks exhibit sharp external contacts and typically contain piercement veinlets of solid sulphide. In many cases, planar fabrics in the blocks of silicate schist are randomly oriented and lack continuity with fabrics in the sulphide matrix (Figure 18f), suggesting that 1) previously deformed inclusions were entrained in the sulphide during primary deposition; 2) primary inclusions and the sulphide were deformed together, but fabric continuity was lost during subsequent internal remobilization; or 3) exotic deformed inclusions were entrained in sulphide during external remobilization beyond the primary layer constraints.

Insofar as it is difficult to envision a process by which large angular blocks of granodiorite were entrained as primary inclusions during sulphide deposition, the first and second options are considered unlikely. The indicated U-Pb age of the granodiorite (i.e., 1.85–1.86 Ga) further suggests that these options are geologically impossible. The third option is fully compatible with the evidence of external sulphide remobilization presented above. Moreover, marginal notes on geological level plans describe complex crosscutting relationships between granodiorite and solid sulphide in the West mine, with widespread evidence for intrusion and stoping of granodiorite by sulphide and vice versa. Speakman et al. (1982) described 'new' (i.e., epigenetic) sulphide lenses in the Main mine that appear to have formed as a result of shear-induced mobilization of chalcopyrite and pyrrhotite into zones of bulk dilation in D_3 shear zones. The authors observed evidence of external mobilization in several locations. In the 25B2 stope on level WM690mL (Figure 8), for example, a 2–3 m thick granodiorite sill is sharply crosscut by the footwall contact of a high-grade (copper-zinc) solid sulphide orebody (Figure 19c). The granodiorite sill is hosted by a thick (>50 m) package of well-layered mafic wacke that is visually indistinguishable from the Powder Magazine unit. In the footwall of the sill, a 10 cm thick layer of pebbly mafic wacke is distinctly graded, indicating that the layering, which dips steeply to the southeast, is primary, although locally highly tectonized. In marked contrast to the footwall elsewhere in the West mine, the mafic wacke in the footwall of the 25B2 stope is visually unaltered and lacks stringer-sulphide mineralization. These aspects of the 25B2 orebody, coupled with its isolated location (Figures 3, 8) and unusual hostrock, are most compatible with emplacement via external remobilization beyond the primary layer constraints of a nearby sulphide lens. External sulphide remobilization was also invoked by Reid (1995) to explain dacite dikes that are crosscut by solid sulphide in the 9B2 stope on level WM590mL.

These examples serve to emphasize the significance of internal and external sulphide remobilization in the Ruttan deposit and the degree to which these processes have apparently influenced the primary geometry and zoning of individual orebodies on a mesoscopic to submacroscopic scale. In the 'Discussion' section, sulphide remobilization is also invoked as a possible explanation for several macroscopic characteristics of the East and West lenses, including the systematic variation of sulphide thickness, metal ratios and mineralization style depending on location in the macroscopic F_2 fold structure.

Structural analysis

Aspects of the structural geology and deformation history of the Ruttan deposit have been briefly described by Speakman et al. (1982), Ames et al. (1990), Reid (1995), Ames (1996), Ames and Taylor (1996), and Schwartz and Brown (2000). Speakman et al. (1982) and Reid (1995) described evidence of meso- to macroscopic isoclinal folding, which they suggested dominates the overall structural style in the mine area. Reid (1995) described an early generation of upright isoclinal folds that plunge shallowly and are overturned to the northwest. On the basis of very limited data, Reid (1995) further suggested that isoclinal refolding of these folds in a constrictional regime produced mine-scale tubular folds, which account for the shoot-like geometry of the principal sulphide orebodies. Although the presence of tubular folds could not be confirmed during the present study, it should nevertheless be noted that Reid (1995) is the only author to have examined the possible influence of macroscopic folding on the deposit geometry. Ames (1996) and Ames and Taylor (1996) described minor Z-shaped folds in the mine area that they attributed to localized deformation along late shear zones, or to early deformation of an unspecified nature, respectively. Ames et al. (1990), in contrast, reported that they did not observe any mesoscopic folds in the mine area, yet also presented compelling evidence of map-scale F_2 folding in the Ruttan Block. Ames and Taylor (1996), in accord with Speakman et al. (1982), suggested that the configuration and geometry of the sulphide orebodies are significantly influenced by late shear zones. Schwartz and Brown (2000) drew a similar conclusion, and further suggested that the lateral margins of the principal orebodies are defined by late shear zones that cut obliquely across section and displace the orebodies in either a normal or a reverse sense.

Sequence of deformation

Overprinting relationships exhibited by mesoscopic deformation structures in the Mine Sequence unit (MSU) indicate a multiphase sequence of ductile deformation, which is provisionally interpreted in the context of four phases (D_1 to D_4; Table 2). Insofar as possible, the structural descriptions of previous workers, outlined above, have been incorporated into the proposed sequence of deformation. As indicated in the preceding descriptions, the distribution and geometry of the principal sulphide lenses are significantly influenced by regional D_2 folding and transposition, followed by distributed D_3 noncoaxial shear.

D_1 deformation structures

Structures that the authors attribute to D_1 deformation are only locally observed in the mine area and typically comprise an early planar fabric element that is preserved in the hinges of F_2 folds. In most instances, the S_1 fabric is a fine-scale penetrative foliation defined by a preferred orientation of fine-grained biotite, sericite and/or chlorite. In fragmental rocks, S_1 is also locally defined by flattened clasts with aspect ratios that range up to 10:1 (Figure 20a). A prominent, millimetre- to centimetre-scale modal layering that consists of rhythmically alternating mica-rich and quartz-rich domains (Figure 20b) is also commonly observed in F_2 fold hinges and, in places, strongly resembles a differentiated crenulation cleavage. The F_1 folds are observed as faint, centimetre-scale isoclines that are refolded in the hinges of F_2 folds and are intrafolial with respect to the modal layering (Figure 19a). In this regard, the modal layering (S_1 in this study) may represent a transposition foliation that overprints one or more older generations of fabric element. It is therefore possible that the fabrics attributed here to D_1 deformation represent more than one generation of structure. Given the intensity of the subsequent deformation and recrystallization,

Table 2: Summary of wallrock deformation structures in the Ruttan deposit.

Deformation phase	Deformation structures	Shortening direction	Regional structure	Age (Ga)	Tectonic significance
D_1	Bedding-parallel S_1 foliation; rare isoclinal F_1 folds	?	Thrust faulting; assembly of structural collage	1.88–1.87	Intraoceanic accretion
D_2	Regional S_2 foliation; downward facing, isoclinal F_2 folds; L^1_2 intersection lineation	NW-SE	Regional-scale folding	1.88–1.87	Accretion of D_1 structural collage to Hearne craton
D_3	Penetrative S_3 foliation in anastomosed, ductile shear zones; rare F_3 folds	E-W	Crustal-scale, greenschist-facies shear zones	1.87–1.85	Orogen-scale east-west shortening during successor- arc magmatism
D_4	Penetrative S_4 in discrete, shallowly south-dipping, ductile shear zones (reverse)	N-S	?	?	Late-orogenic shortening

however, it was not possible to resolve a pre-D_1 structural history for the MSU.

D_2 deformation structures

Deformation structures attributed to D_2 deformation are regionally pervasive in at least the northern portion of the Ruttan Block, and record isoclinal folding and transposition in the Mine Sequence and Powder Magazine units. The S_2 planar fabric is pervasive, strikes northeast to east-northeast and dips steeply to the southeast. In F_2 fold hinges, S_2 is a spaced (1–10 mm) crenulation cleavage that is oriented orthogonal to S_1 and is axial planar to open to tight, generally symmetric microfolds of the S_1 fabric (Figures 5c, 20a). Toward the F_2 fold limbs, the separation between the cleavage planes decreases and S_2 grades into a penetrative transposition foliation defined by medium- to coarse-grained biotite, sericite and chlorite. The associated F_2 microfolds are characteristically intrafolial isoclines that range from markedly asymmetric, to symmetric and rootless. In these areas, the S_2 transposition fabric is a composite S_{1-2} that forms a pronounced tectonite layering (Figure 4). In the Powder Magazine unit, this layering represents strongly transposed bedding; in the Mine Sequence unit (MSU), it appears to represent either bedding or an earlier tectonite fabric.

In the East and West lenses, the distribution of solid and near-solid sulphide defines a macroscopic F_2 fold in the medial portion of the MSU, which is transected and locally displaced by D_3 shear zones (Figure 2). As with the S_2 fabric, the character of mesoscopic F_2 folds is variable, depending on location within this macroscopic F_2 fold structure. Parasitic F_2 folds in the hinge are open to tight and generally symmetric (Figure 20b), whereas those on the limbs are typically tight to isoclinal, and rootless and intrafolial with respect to the D_2 tectonite fabric (Figure 20c). Trains of asymmetric F_2 folds are locally preserved on the fold limbs, and their sense of asymmetry typically corresponds to their position within the macroscopic F_2 structure. The F_2 folds consistently plunge toward the east-southeast at steep to moderate angles. The macroscopic F_2 hinge defined by the major ore shoots in the East lenses appears to be slightly curvilinear (Figure 3) and may have rotated through as much as 55°; however, no examples of sheath or tubular F_2 folds were observed. Younging criteria in the JS lens indicate that the F_2 folds are downward-facing structures, which suggests structural overturning prior to D_2 deformation.

The intersection between S_1 and S_2 produces a prominent lineation (L^1_2) that is pervasive in the mine area and plunges toward the east-southeast at steep to moderate angles. In the East lenses on level MM080mL, changes in S_1-S_2 vergence between the L and J lenses (Figure 21) indicate the location of the axial trace of the macroscopic F_2 fold. Similar changes in S_1-S_2 vergence in core from drillhole UR1505 (Figure 17) pinpoint the location of the fold hinge on level MM660mL. In the hinge of the fold, the L^1_2 lineation is coaxial with a pronounced elongation lineation that is developed on a variety of scales. In the footwall of the JS lens on level MM800mL (also the J lens on level MM730mL), this lineation is manifested as discrete, pencil-shaped aggregates of sulphide minerals that plunge steeply to the east-southeast. The axial ratios of these aggregates are typically 10:1:1 (X:Y:Z) or greater and thus define prolate ellipsoids. Locally, the aggregates are arranged in distinct linear trains, which define a subtle, centimetre-scale layering orthogonal to the finely spaced S_2 crenulation fabric in the host quartz-sericite schist. In the equivalent structural location on level MM370mL (east footwall drift), the L^1_2 lineation is coaxial with cylindrical boudins of diabase up to 1 m in diameter. These observations are interpreted as indicating that the elongation lineation formed in response to layer-parallel extension in the S_1 plane around the arc of the macroscopic hinge during F_2 folding (i.e., longitudinal strain). No examples of a stretching lineation were observed in the Ruttan deposit or the MSU.

Ames et al. (1990) indicated that the bedding-parallel S_1 foliation northeast of the Ruttan deposit is consistently overprinted at a counter-clockwise angle by S_2, and suggested that the deposit is located on the limb of a map-scale F_2 fold. The consistent Z-asymmetry of early folds in the mine area (Ames, 1996; Ames and Taylor, 1996) is compatible with the S_1-S_2 vergence. Along strike northeast of the mine, Baldwin (1988) mapped a macroscopic, Z-asymmetric interfingering of the Mine Sequence and Mill Pond units (Figure 1) but did

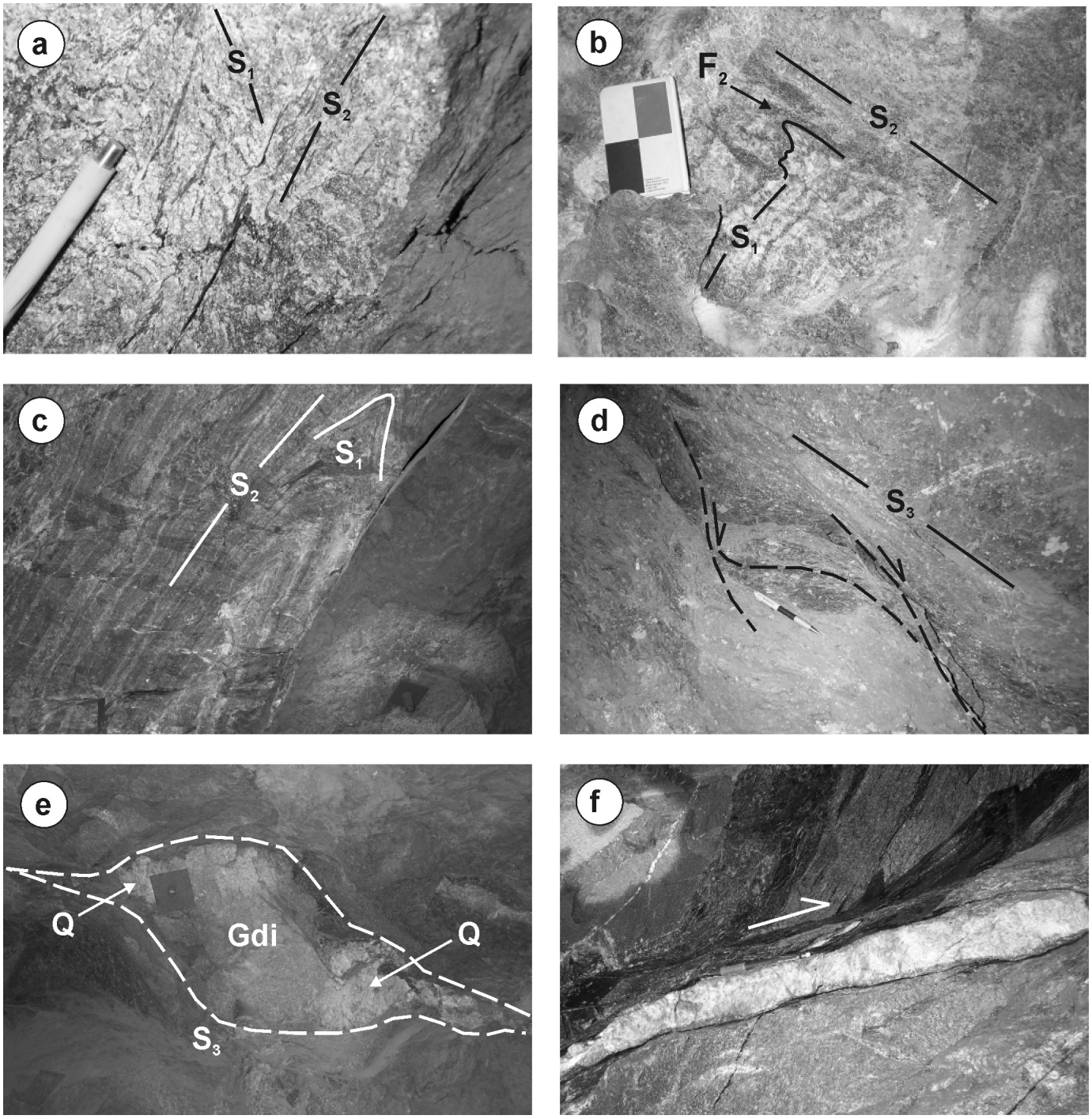

Figure 20: *Photographs of wallrock deformation structures, Ruttan deposit:* ***a)*** *S_1 fabric, defined by flattened clasts, overprinted by the S_2 crenulation cleavage in the hinge of the macroscopic F_2 fold in the East lenses, wall exposure (facing west), level MM370mL, east footwall drift;* ***b)*** *symmetric F_2 folds in the hinge of the macroscopic F_2 fold, between the L and J lenses, wall exposure (facing north), level MM260mL, L3 stope, No. 2 drawpoint;* ***c)*** *isoclinal F_2 fold on the south limb of the macroscopic F_2 fold in the East lenses, back exposure (facing west), level MM660mL, hangingwall crosscut; rock-bolt plate (lower right) is 15 cm square;* ***d)*** *large-scale asymmetric shear bands indicating dextral-normal oblique slip in Art's Shear Zone, wall exposure (looking east), level MM730mL, west footwall drift;* ***e)*** *large asymmetric boudin of granodiorite (Gdi) in the North Wall Shear Zone, in the footwall of the B lens, back exposure, (facing northwest), level WM690mL, footwall drift at 17B stope; rock-bolt plate is 15 cm square; note the quartz-filled strain shadows (Q), the asymmetry of which indicates dextral shear when looking down dip;* ***f)*** *shallow-dipping D_4 shear zone cutting steep S_2 foliation, wall exposure (facing west), level WM790mL, access ramp; asymmetric quartz boudins indicate top-to-the-north shear (pencil for scale on upper contact of the quartz vein).*

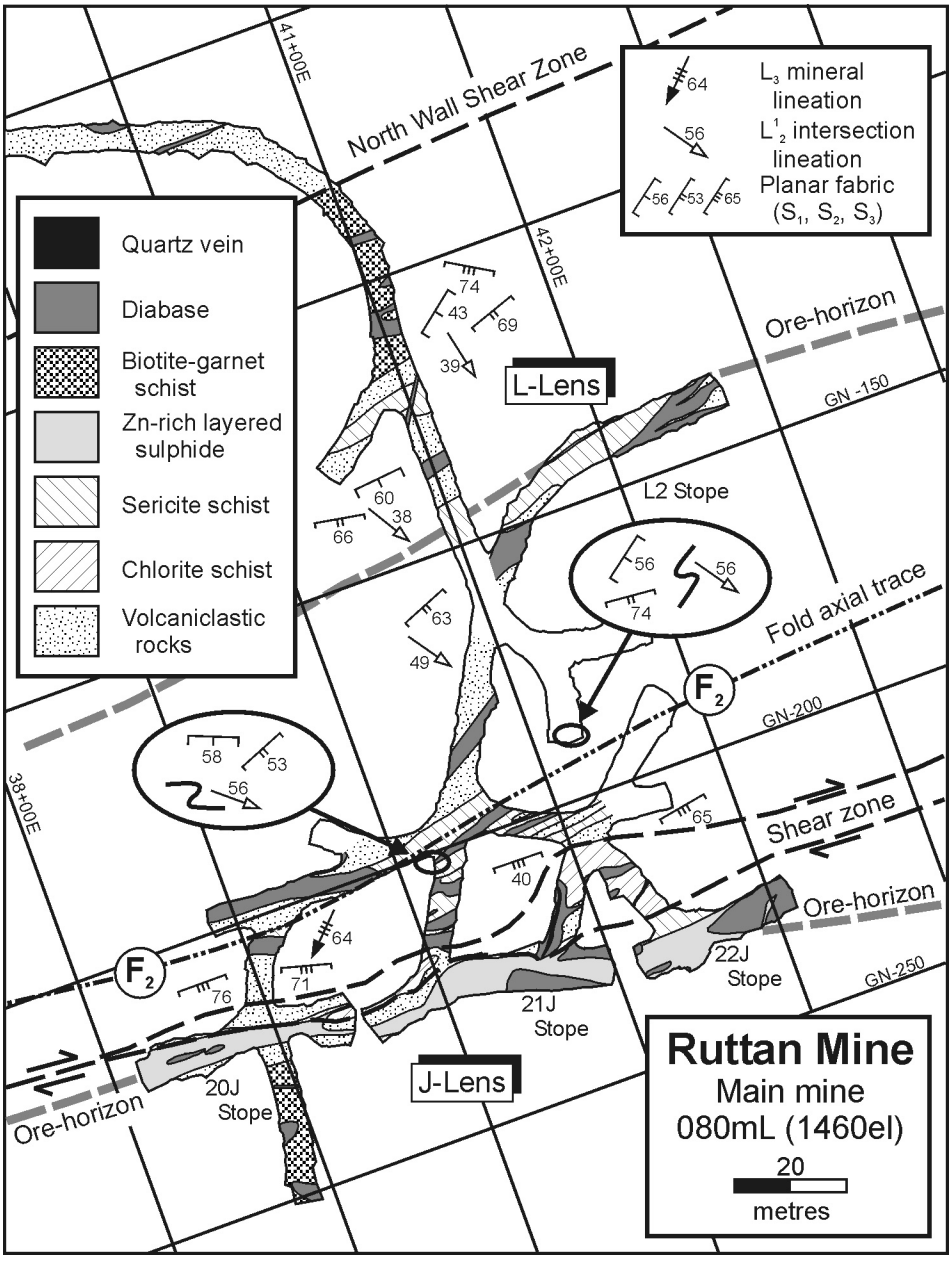

Figure 21: *Simplified geological plan of level MM080mL, Ruttan deposit, based on mapping by mine geologists and the authors. Note the change in vergence of the F_2 microfolds on either side of the isoclinal, macroscopic F_2 fold hinge.*

not provide an explanation for the map pattern. A similar map pattern is evident immediately east and southeast of the open pit, in the location where a distinct unit of buff-weathering, quartz-phyric, felsic volcaniclastic rocks (e.g., Gale, 2003) extends to the southwest into the Powder Magazine unit (Figure 2). Although mapped by Ames and Scoates (1992) as a 'quartz-plagioclase porphyry dike' that ranges from 120 to 170 m thick and abruptly terminates 200 m south of the vent-raise for the Main mine, the few available surface exposures of this unit are characterized by coarse fragmental textures and a diffuse, northeast-trending layering that is defined by subtle variations in the proportion of quartz crystals. In accord with Rayner and Corrigan (2004), the authors correlate these rocks with the 'upper felsic volcaniclastic unit' of Ames (1996), and thus interpret the map pattern to indicate a macroscopic Z-asymmetric interfingering of the Powder Magazine and Mine Sequence units that mimics that mapped by Baldwin (1988). These features are attributed to isoclinal folding of the MSU by a train of macroscopic, Z-asymmetric F_2 folds (Figure 2). Coupled with the available younging criteria, this asymmetry indicates that the Ruttan deposit is situated on the north limb of a map-scale F_2 syncline (e.g., Ames et al., 1990), which is downward-facing (i.e., antiformal) and closes to the northeast. Interestingly, the map pattern appears to be locally mimicked by the north contact of the Corner Lake pluton south of the open pit (Figure 2). Although this is unexposed on surface or underground, the authors speculate that this results from magmatic emplacement of the diorite around a pre-existing F_2 fold hinge, as opposed to F_2 folding of the diorite. This interpretation is supported by the contact relationships observed in drillhole

UR1505, which indicate that the F_2 fold limb is crosscut by the diorite (Figure 17).

D_3 Deformation

The D_3 deformation structures in the mine area are associated with a prominent network of anastomosed ductile shear zones, which include the NWSZ, ASZ and ESZ. Individual shear zones in this network range up to 30 m thick and are typically manifested as discrete, laterally continuous zones of chlorite-biotite schist, near-solid sulphide schist and silicate-sulphide schist or tectonite. The shear zones generally dip toward the southeast at moderate to steep angles, although the orientation of individual zones is highly variable and several exhibit a pronounced S-sigmoidal geometry in both plan and section (looking east). This geometry is most prominently illustrated on a macroscopic scale by the ESZ and ASZ, which exhibit systematic changes in orientation along strike (Figure 2), from steeply south-southeast dipping at their lateral tips to moderately southeast dipping in their medial portions. These shear zones appear to represent hangingwall splay structures off the NWSZ, which dips steeply to the south-southeast and defines a footwall 'master structure' to the shear-zone network (e.g., Speakman et al., 1982). Mesoscopic examples of this geometry are best observed in the West mine, where discrete zones of chlorite and sulphide-silicate schist splay off the hangingwall of the NWSZ and cut across section toward the southwest into the hangingwall of the B lens. The offset and duplication of the B lens on level WM590mL (Figure 9) is likely a manifestation of this structural geometry. To the south, the authors speculate that these shear zones merge into the contact between the Mine Sequence and Powder Magazine units (Figure 2).

In the central portions of the shear zones, the S_3 planar fabric is typically a penetrative foliation defined by a preferred alignment of medium- to coarse-grained chlorite, biotite and elongate sulphide minerals (principally pyrite). Along the margins of the shear zones, the S_3 foliation clearly overprints the S_2 fabric in the adjacent, generally more siliceous wallrocks. In some cases, the margins of the shear zones are remarkably sharp and the S_2 fabric in the wallrocks is sharply truncated by chlorite schist. In other cases, the margins of the shear zones are gradational through a metre-scale zone of partitioned S_3 fabric development that contains lenticular domains of the siliceous, S_2-foliated wallrock. In these locations, southeast-plunging F_3 folds of the S_2 fabric are locally observed. These folds are open to tight, with a weak, spaced axial-planar S_3 fabric and a pronounced Z-asymmetry. Veinlets and pods of *durchbewegt* sulphide-silicate schist (pyrrhotite-chalcopyrite-chlorite±anhydrite) are characteristic of the D_3 shear zones, as are boudinaged quartz ± chlorite, chalcopyrite or anhydrite veins up to 1.5 m thick.

The D_3 shear zones are characterized by an abundance of well-developed asymmetric fabrics, which include oblique internal foliations (Figure 20d), S-C fabrics (Figure 18d), shear bands (Figure 18c), foliation fish, porphyroclast systems (Figure 20e), and back-rotated layer and boudin segments. In most localities, a linear fabric element is not well developed and the slip vector for individual shear zones is assumed to be roughly orthogonal to the line of intersection of the planar fabric elements that define the asymmetric fabrics. In all cases, the asymmetric fabrics indicate dextral shear with a variable component of normal oblique slip. This kinematic framework is compatible with the bulk geometry of the D_3 shear-zone network. The poles to the S_3 foliation in D_3 shear zones throughout the deposit define a partial girdle (Figure 22), the best-fit great circle to which is considered to roughly approximate the bulk symmetry-plane of the shear-zone network. The β-axis of the network, as indicated by the pole to the bulk symmetry-plane, plunges moderately to the east-southeast, subparallel to the general elongation of the Ruttan orebodies. Ideally (i.e., assuming a monoclinic bulk symmetry), the bulk slip-vector should be orthogonal to the β-axis and roughly parallel to the intersection of the bulk symmetry-plane with the boundary of the shear-zone network. Although the boundary of the D_3 shear-zone network is poorly constrained, the available data suggest a bulk slip-vector that plunges shallowly southwest (i.e., mainly strike-slip shear; Figure 22). However, the orientation of the mineral lineation in the D_3 shear zones is quite variable (Figure 22), which may indicate 1) the presence of a pre-existing lineation that was variably reoriented during D_3 deformation; 2) a triclinic symmetry (e.g., Lin et al., 1998) for the D_3 shear-zone network; or 3) dip-slip reactivation of the D_3 shear zones, perhaps as a consequence of D_4 subhorizontal shortening (*see* below). The available data are presently insufficient to differentiate between these possibilities.

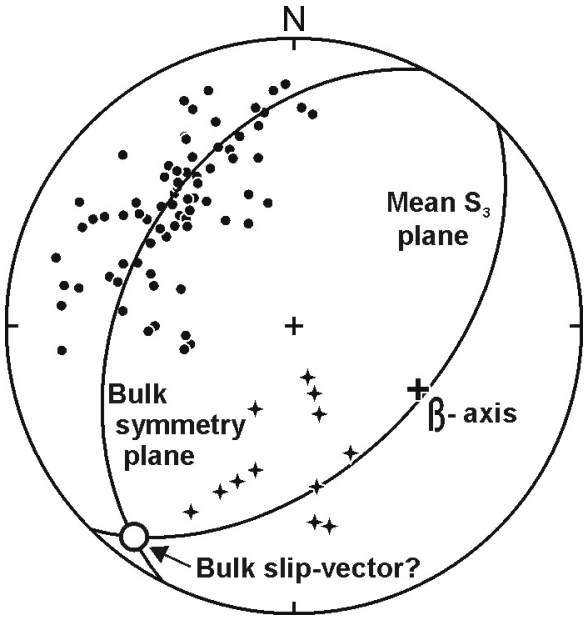

Figure 22: *Equal-area, lower-hemisphere stereographic projection of poles to the measured S_3 foliation (solid circles; N = 74) in D_3 shear zones throughout the Ruttan deposit, showing the mean S_3 plane, the bulk symmetry-plane of the shear-zone network, the possible bulk slip-vector (open circle), and the β-axis (heavy cross). The crosses indicate mineral lineations (chlorite or biotite; N = 12) in the D_3 shear zones.*

In the D_3 shear zones, the penetrative S_3 foliation is only slightly warped around the margins of garnet, cordierite, staurolite and anthophyllite porphyroblasts, suggesting that porphyroblastesis and the metamorphic peak were late kinematic with respect to D_3 deformation. In many locations, the S_3 foliation has been partially obliterated by late-kinematic annealing recrystallization, which has produced a coarse-grained, locally granoblastic texture in the chlorite-biotite schist. This annealing recrystallization is particularly intense and pervasive in the western portion of the West mine, close to the Brehaut Lake pluton. In this area, granodiorite dikes that are presumed to be associated with the Brehaut Lake pluton account for up to 50% of the section and form an irregular macroscopic stockwork and southeast-trending dike swarm. In the footwall of the B lens, granodiorite dikes and D_3 shear zones exhibit complex mutual overprinting relationships, with local evidence to suggest pre- or early-D_3 (Figure 23a), syn-D_3 (Figure 23b) and post-D_3 (Figure 23c) dike emplacement. These relationships, coupled with the U-Pb evidence for slightly older inherited components in the late-kinematic granodiorite dike, suggest protracted granodiorite emplacement. The overall weight of evidence, however, appears to support mainly syn- to late-D_3 dike emplacement, particularly in light of the late-kinematic relative timing of annealing recrystallization and porphyroblastesis in the thermal aureole of the Brehaut Lake pluton.

D_4 Deformation

Deformation structures attributable to D_4 deformation are only locally observed in the Ruttan mine and apparently had little influence on the deposit geometry. The best examples of D_4 structures are observed mainly in the West mine and appear to record late-tectonic subhorizontal compression. In the deeper levels of the West mine, the D_4 structures consist of a series of widely spaced, discrete ductile shear zones that are typically 0.1–0.5 m thick. These shear zones dip very shallowly (ca. 30°) to the southeast or south and contain a penetrative foliation defined by chlorite and biotite that sharply crosscuts the steeply dipping S_2 or S_3 fabrics in the wallrocks (Figure 20f). In many locations, these shear zones contain laminated, strongly sheared quartz veins. Asymmetric fabrics and back-rotated boudin segments indicate top to the northwest (thrust-sense) shear. In the Main mine, subhorizontal tension gashes that overprint the S_3 foliation in the ESZ on level MM370mL (Figure 18e) also suggest subhorizontal shortening and are attributed to D_4 deformation.

Discussion

Regional tectonic implications

The kinematic and tectonic significance of D_1 deformation are poorly constrained. Structural facing criteria indicate that the Ruttan deposit is located on the north limb of a regional-scale, antiformal F_2 syncline, which suggests that D_1 deformation may have involved early structural overturning, perhaps associated with thrust faulting and nappe-style folding (i.e., horizontal tectonics). This style of early deformation has previously been proposed for the Lynn Lake–Leaf Rapids

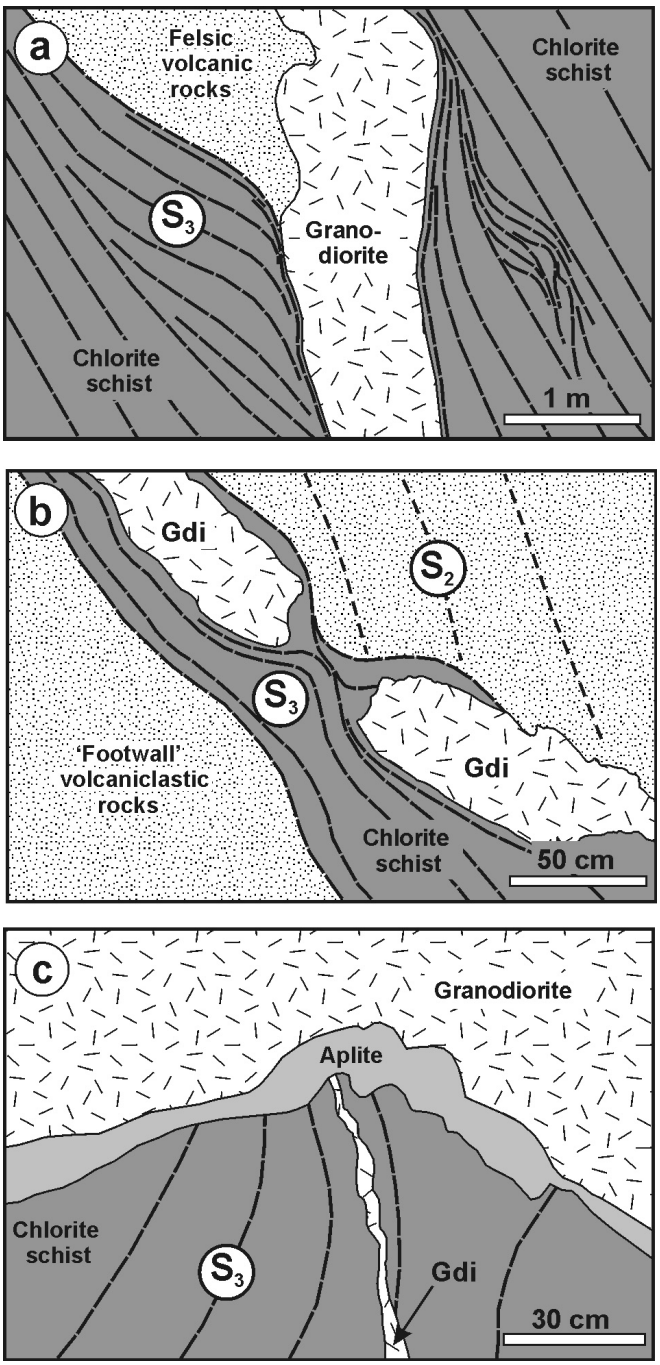

Figure 23: *Simplified sketches (from photographs) of observed overprinting and crosscutting relationships between granodiorite dikes and D_3 shear zones (chlorite schist) in the B lens footwall, West mine, Ruttan deposit:* ***a)*** *apparent pre- or early-D_3 granodiorite dike, wall exposure (facing northeast), level WM440mL, 4B2 stope, west drawpoint;* ***b)*** *apparent syn-D_3 granodiorite dike, wall exposure (facing northeast), level WM790mL, access ramp; note that the dike is boudinaged in S_3, yet discordantly cuts S_2 and S_3 in the lower right portion of the sketch;* ***c)*** *apparent post-D_3 granodiorite dike, wall exposure (facing southwest), WM440mL, 4B2 stope, east drawpoint; the granodiorite sample for U-Pb geochronology was collected at this site; situated 15 m along strike to the west-southwest of the locality illustrated in part a, within the same D_3 shear zone. Abbreviation: Gdi, granodiorite.*

Domain and is thought to have accompanied the assembly of diverse, 1.91–1.88 Ga tectonostratigraphic assemblages into an intraoceanic structural collage near the north margin of the Trans-Hudson Orogen (Zwanzig et al., 1999; Beaumont-Smith and Böhm, 2002, 2003). Intraoceanic assembly and final accretion of this structural collage to the Hearne craton margin are constrained to 1.88–1.87 Ga (Gordon et al., 1990; Zwanzig et al., 1999; White et al., 2000) by crosscutting plutons associated with continental-arc and successor-arc magmatism at ca. 1.87–1.85 Ga (Bickford et al., 1990). On the opposing (south) margin of the orogen, the well-documented Amisk collage (Flin Flon belt) is also thought to record 1.88–1.87 Ga intraoceanic accretion of 1.92–1.88 Ga tectonostratigraphic assemblages (Lucas et al., 1996; Stern et al., 1999), likely in association with low-angle D_1 thrust faulting (Ryan and Williams, 1999). In the Rusty Lake belt, arc-tholeiitic and calcalkalic volcanic rocks of the Mine Sequence unit (MSU) appear to be tectonically juxtaposed across the Mill Pond Shear Zone with ocean-floor basalt of the Mill Pond unit (Ames, 1996). Contact relationships and surface map patterns likewise suggest a tectonic contact between the Mine Sequence and Powder Magazine units, which is overprinted by F_2 folds. On this basis, the authors speculate that D_1 deformation records the tectonic assembly of the supracrustal units into a structural collage that was subsequently stitched by the ca. 1.865–1.85 Ga Brehaut Lake pluton. Given the available age constraints, it is permissible that D_1 deformation is related to intraoceanic accretion at 1.88–1.87 Ga.

The D_2 deformation structures are pervasive in at least the northern portion of the Ruttan Block and include a penetrative, northeast-trending, S_2 transposition fabric that is axial planar to upright, tight to isoclinal F_2 folds that plunge steeply east. In this area, the vergence of macroscopic F_2 folds and facing criteria indicate that the Ruttan deposit is situated on the north limb of a map-scale F_2 syncline that faces downward and closes to the northeast. These structures are crosscut by granodiorite dikes associated with the Brehaut Lake pluton, suggesting a minimum age of ca. 1.852 Ga for D_2 deformation. On a regional scale, continued or renewed shortening of the D_1 structural architecture, perhaps as a consequence of accretion of the structural collage to the south margin of the Archean Hearne craton, provides a plausible explanation for D_2 deformation that is compatible with the general style and relative timing of the associated deformation structures.

In the Lynn Lake belt, D_2-generation structures are also regionally developed and are interpreted to record a progressive transition from early fold-dominated deformation to later shear-zone–dominated deformation, in a regional regime of dextral transpression (Beaumont-Smith and Böhm, 2002, 2003). In this model, F_2 folds are thought to have initiated as upright, subhorizontal, open structures developed within a shallow-dipping, macroscopic enveloping surface that records horizontal tectonics during development of the D_1 crustal architecture. With continued shortening, D_2 strain was preferentially partitioned into dextral transpressive shear zones, which include the crustal-scale Johnson Shear Zone along the south margin of the belt, with progressive steepening of the F_2 fold hinges in these higher strain domains. As described by Beaumont-Smith and Böhm (2002, 2003), however, these D_2 structures overprint 1.87–1.85 Ga plutons and the unconformably overlying fluvial-alluvial siliciclastic rocks of the ca. 1.85–1.84 Ga Sickle Group, which indicates that the regional D_2 deformation in the Lynn Lake belt was probably unrelated to the early (1.88–1.87 Ga) accretionary history of the Lynn Lake–Leaf Rapids Domain. Hence, the available time constraints do not support a regional correlation of D_2 deformation, despite the roughly similar D_2 structure of the Lynn Lake and Rusty Lake belts.

In the Ruttan mine area, D_3 deformation structures define a northeast-trending, anastomosed network of ductile shear zones, which records dextral transcurrent shear, with a variable component of normal oblique slip. Overprinting relationships indicate that D_3 deformation was roughly coeval with 1.87–1.85 Ga successor-arc magmatism, as represented by the Brehaut Lake and Corner Lake plutons, and largely predates the local amphibolite-facies metamorphic peak in the associated thermal aureoles. The geometry and kinematics of the shear-zone network suggest roughly east-west shortening (present coordinates) during D_3 deformation. Along strike to the northeast, the regional-scale Vol Fault crosscuts the D_2 structural grain and appears to be stitched by the Brehaut Lake pluton (Figure 1), which suggests that D_3 deformation may also be manifested on a regional scale. In this regard, it is noteworthy that evidence of regional east-west shortening is observed in the eastern Amisk collage (Ryan and Williams, 1999) and likewise appears coeval with ca. 1.87–1.85 Ga successor-arc magmatism and contact metamorphism (Lucas et al., 1996). These data provide cryptic evidence of orogen-scale east-west shortening during successor-arc magmatism in the Trans-Hudson Orogen.

Regional aeromagnetic patterns, although partially obscured by successor-arc plutons, indicate that the Vol Fault may merge along strike to the northwest with the Johnson Shear Zone along the south margin of the Lynn Lake belt. It is therefore possible that the Lynn Lake belt and that portion of the Rusty Lake belt south of the Vol Fault were originally contiguous, and thus represent segments of a single, regionally extensive structural collage that was truncated and displaced by the crustal-scale 'Johnson-Vol' structural break. Although the kinematics of the Vol Fault are unknown, the regional northwest trend of this linear structure suggests that it may have been favourably oriented for sinistral transcurrent shear in a regime of east-west shortening (present coordinates) during D_3 deformation. Thus, any displaced portion of the VMS-hosting Ruttan Block, if it in fact exists, might be expected to occur north of the Johnson-Vol break, northwest or west of the Ruttan mine.

The only other significant VMS deposit discovered to date in the Lynn Lake–Leaf Rapids Domain is the Fox Lake deposit, which is situated 120 km west-northwest of the Ruttan deposit, near the southwest end of the Lynn Lake belt (Figure 1). Although a detailed comparison is beyond the scope of this study, several characteristics of the Fox Lake deposit are analogous to the Ruttan deposit, including 1) the deposit hostrocks, which comprise a thick package of intercalated arc-tholeiitic and calcalkalic basalt and andesite, with minor dacite and rhyolite (Lustig, 1979; Gilbert et al., 1980; Olson, 1987; Zwanzig et al.,

1999); 2) the overall tectonostratigraphic setting, in which the hostrocks are bounded to the north by a section of MORB-like pillowed basalt and to the south by a thick succession of greywacke-mudstone turbidite (Gilbert et al., 1980; Zwanzig et al., 1999); 3) the spatial association of the dacitic volcanic rocks with extensive zones of cordierite-anthophyllite and cordierite-biotite-sillimanite alteration (Lustig, 1979; Gilbert et al., 1980); 4) the presence of early isoclinal folds and intense transposition fabrics in the mine succession (Lustig, 1979; Gilbert et al., 1980; Olson, 1987; Beaumont-Smith and Böhm, 2002); and 5) the overall metal ratios and low grade of the sulphide mineralization (1.82 wt.% Cu, 1.78 wt.% Zn, negligible Pb and minor Au and Ag; Olson, 1987). In addition, Beaumont-Smith and Böhm (2002) reported a U-Pb zircon age of 1891 ±2 Ma for dacite along strike to the east of the Fox Lake deposit, which overlaps the probable age of felsic volcanism associated with the Ruttan deposit (i.e., 1.91–1.88 Ga; Rayner and Corrigan, 2004). These similarities, in conjunction with the proximity of the VMS deposits to the Johnson-Vol break, suggest that it may be possible to establish a direct correlation between the Rusty Lake and Lynn Lake belts. Although highly speculative, this correlation could help explain the curious fact that the Fox Lake and Ruttan deposits are both apparently solitary and occur within fault-truncated tectonostratigraphic sections on the extremities of their respective supracrustal belts.

The latest increment of deformation (D_4) in the Ruttan mine area appears to record subhorizontal, roughly north-south shortening of the D_2-D_3 structural architecture. Unfortunately, since the absolute timing of this deformation remains unknown, it is not possible to provide any insight into the regional significance of the D_4 deformation.

Implications for stratigraphic models of the MSU

Current models for the stratigraphy and genesis of the Ruttan deposit are invariably predicated on the inference of a consistently upright, south-younging stratigraphy for the MSU (e.g., Speakman et al., 1982; Ames, 1996; Ames and Taylor, 1996; Barrie and Taylor, 2001; Gale, 2003). This inference, which is inextricably linked to the present understanding of the Ruttan VMS system, is based on three lines of evidence:

- contact relationship between the Mine Sequence unit and the primarily south-younging sedimentary rocks of the Powder Magazine unit, which is inferred to be conformable
- distribution of chlorite (± biotite, cordierite, anthophyllite, garnet) alteration in the MSU, which is thought to define a footwall alteration zone
- bulk-scale patterns of metal zoning and mineralization style in the deposit, which are interpreted to indicate a consistent younging direction to the south in the MSU.

The structural model presented in this report, however, significantly complicates this simplistic stratigraphic framework, as it requires large-scale structural overturning within the deposit, on the short limb of the macroscopic, Z-asymmetric F_2 fold. This important discrepancy is addressed by examining each line of evidence in detail.

Contact relationship between the Powder Magazine and Mine Sequence units

As mentioned previously, the available evidence is interpreted to indicate a wholly tectonic contact relationship between the Mine Sequence (MSU) and Powder Magazine units. This evidence includes 1) the angular discordance observed between layers in the Powder Magazine unit and the upper contact of the J lens on level MM490mL, coupled with the absence in this location of the upper felsic volcaniclastic unit of the MSU; 2) the U-Pb geochronological data of Ames et al. (2002) and Rayner and Corrigan (2004), which suggest that the Powder Magazine unit was not derived from the immediately underlying MSU; and 3) the surface map patterns northeast of the mine, which clearly indicate that the south contact of the MSU cuts discordantly across the section of the Powder Magazine unit. For these reasons, the authors do not accept the Mine Sequence and Powder Magazine units as a conformable stratigraphic succession, and therefore consider younging criteria in the latter irrelevant to any discussion of younging direction(s) in the former.

Distribution of chlorite alteration

Several authors have argued that the laterally extensive zones of chlorite (± biotite, cordierite, anthophyllite or garnet) schist in the footwall of the Ruttan deposit record syngenetic alteration in a seafloor hydrothermal conduit system, and have used this interpretation as evidence to suggest a south-younging stratigraphy for the MSU (e.g., Ames, 1996; Barrie and Taylor, 2001; Gale, 2003). The distribution of the chlorite alteration, however, is not as straightforward as this simplistic model would suggest. In the West mine, the B lenses are enveloped by laterally extensive zones of chlorite-biotite± cordierite±anthophyllite±garnet schist (Ames and Taylor, 1996), and a similar relationship is observed in the Main mine, where the West lenses are tightly bounded by thick zones of chlorite-biotite±cordierite schist that coincide with the ESZ and ASZ (Speakman et al., 1982). Ames and Scoates (1992) and Ames (1996) documented extensive zones of cordierite-chlorite alteration in the footwall and hangingwall of the East lenses and noted that individual sulphide orebodies are locally enveloped by this alteration. Hence, chlorite alteration is not restricted to the footwall of the Ruttan deposit and, in the case of the JS and B lenses, is demonstrably well developed in the stratigraphic hangingwall of the sulphide mineralization. As described by Goodfellow et al. (1993), actively forming VMS deposits in the Middle Valley of the Juan de Fuca ridge are locally overlain by concordant zones of intense magnesian (talc) alteration and are thus characterized by an 'inverted' pattern of hydrothermal alteration that is clearly primary. In the case of the Ruttan deposit, it remains unclear to what extent the distribution of chlorite is related to syngenetic hydrothermal processes, or to what extent it might be related to syntectonic (i.e., epigenetic) metasomatism in the major D_3 shear zones that typically coincide with the most intense, laterally extensive zones of chloritization. Regardless, the authors do not believe that the distribution of chlorite provides a reliable indicator of younging direction in the MSU.

Patterns of metal zoning and mineralization style

Several authors (e.g., Speakman et al., 1982; Ames and Taylor, 1996; Barrie and Taylor, 2001; Gale, 2003) have asserted that the Ruttan deposit is characterized by a relatively copper-enriched footwall and zinc-enriched hangingwall, and thus exhibits a 'normal' (i.e., upright) pattern of metal zoning that conforms closely to classic models of VMS deposition. On the scale of the entire deposit, however, drillhole assay data provide little evidence to support this assertion. Continuous assay profiles across the thickest (up to 90 m) sulphide orebodies in the West and East lenses do not exhibit any systematic variations in metal ratios or content, and instead indicate highly erratic, though generally elevated copper, typically with negligible zinc. High-grade zinc values are locally observed, but tend to coincide with particularly high-grade copper, and there is no evidence to suggest relative zinc enrichment in the hangingwall. Indeed, the immediate footwall of these 'copper-rich' orebodies hosts the B lens, which contained intervals of high-grade zinc ore that were among the richest in the entire deposit. Along strike to the east, the footwall of the East lenses is similarly marked by the zinc-rich L lens. Notwithstanding these examples, a 'normal' pattern of metal zoning is evident in assay profiles across portions of the J, JS and B lenses, and this zoning is locally evident in multiple drillholes and across more than one section. Locally, the JS and B lenses also exhibit a clear gradation from footwall copper-rich stringer ore, through medial copper-rich massive ore, to hangingwall zinc-rich layered ore, which indicates that these lenses are likely upright. On the basis of these limited data, however, the authors do not consider it reasonable to conclude that the entire deposit is upright, particularly given the structural evidence to the contrary. Although no clear examples of overturned sulphide lenses could be identified on the basis of zoning patterns, it should be pointed out that the upright lenses occur on the long limbs of the macroscopic, Z-asymmetric F_2 fold. In this regard, the apparent absence of inverted zoning patterns on the highly attenuated short limb of the F_2 fold may simply be a function of D_2 transposition and remobilization of sulphide (*see* below).

On the basis of the foregoing, the authors conclude that the only reliable indicators of younging direction in the MSU are provided by patterns of mineralization style in the JS and B lenses; hence, the proposed structural model is fully compatible with the available younging criteria. Despite the lack of clear examples of overturned younging criteria, the structural model predicts that substantial younging reversals must be present in the MSU, and thus provides a significantly improved, though more complex, framework in which to understand the stratigraphy and genesis of the Ruttan deposit.

Of particular significance in this regard are the implications of the structural model for the ongoing studies of rare-earth-element (REE) and trace-element systematics in the Ruttan VMS system, which are invariably predicated on a consistent younging direction throughout the examined stratigraphic intervals (e.g., Barrie and Taylor, 2001; Gale and McClenaghan, 2002; Gale et al., 2002; Gale, 2003). By analyzing samples of ore-equivalent strata intersected in surface drillholes along strike northeast of the deposit, as well as samples obtained from potentially correlative strata in the southern Ruttan Block, a major objective of these studies is to determine the viability of using REE geochemistry (particularly Eu) as a vector to known VMS mineralization, and thus provide a potential tool to evaluate any residual mineral potential in the mine area. In order to be practical from an exploration perspective, however, the REE data must be interpreted in the context of a realistic stratigraphic model that takes into consideration the structural context of the sampled intervals.

As an example of the potential pitfalls associated with a layer-cake stratigraphic approach, one need only consider RPE89-12, which is one of five drillholes included by Gale (2003) in a stratigraphic and REE geochemical analysis of the MSU along strike northeast of the Ruttan deposit. Hole RPE89-12 was drilled from surface on section 46+00E to test the eastern strike extent of the East lenses between the open pit and the shaft, and thus provides a complete section across the southern hinge of the macroscopic isoclinal F_2 fold in the MSU. In the drillcore, the hinge of the fold is observed at 161.0 m downhole and is clearly indicated by the near orthogonal overprinting of an early planar fabric (S_1; defined by flattened clasts at a low angle to the core axis) by a well-developed crenulation cleavage (S_2; defined by foliated biotite at a high angle to the core axis). When projected 120 m along strike to the west-southwest, the position of the fold hinge corresponds to that of the macroscopic F_2 fold mapped on level MM080mL in the East mine (Figure 22). Significantly, RPE89-12 also intersected two thin horizons of sphalerite-rich near-solid sulphide (at 38.7–40.6 m and 250.9–252.1 m downhole), which are symmetrically disposed about the fold hinge and correlate well with the position of the J and L lenses, respectively, on level MM080mL. Hole RPE-89-12 also contains two distinctive intercepts of light grey, fine- to medium-grained, biotite-chlorite schist that contain evenly distributed idioblastic porphyroblasts of magnetite up to 7 mm across. These intercepts (at 97.6–123.5 m and 185.1–219.5 m downhole) are also symmetrically disposed about the fold hinge. Although Gale (pers. comm., 2002) also noted the symmetric repetition of rock types in RPE89-12, the corresponding REE data were nevertheless interpreted by Gale (2003) in the context of an upright stratigraphic succession. In the authors' opinion, however, the failure to incorporate this major younging reversal into the interpretation of the downhole geochemical data calls into question the validity of the conclusions drawn by Gale (2003) with respect to REE systematics in the MSU.

Orebody controls and exploration implications

As described previously, the principal sulphide lenses in the Ruttan deposit exhibit systematic lateral variations in thickness, metal ratios and style of mineralization, depending on location within the macroscopic, Z-asymmetric, F_2 fold structure in the MSU. Understanding the genesis of these lateral variations is critical to understanding the fundamental controls on the Ruttan deposit and is therefore also important for assessing the residual exploration potential of the southwest Rusty Lake belt.

On the long limbs of the fold, solid and near-solid sulphide

are disposed in laterally and vertically continuous, tabular orebodies of relatively uniform thickness (typically 10–15 m). These orebodies (e.g., the western B lens and eastern portions of the J and JS lenses) locally exhibit patterns of metal zoning and mineralization style that are interpreted to be primary (e.g., Speakman et al., 1982; Ames, 1996; Barrie and Taylor, 2001; Gale, 2003). On the northern long limb of the fold, the eastern B lens locally displays similar patterns, but is disposed in a series of discrete, lenticular ore shoots along the NWSZ that plunge steeply east and exhibit evidence of back rotation in a kinematic regime of dextral strike-slip shear (Figure 16). The northern hinge and short limb of the fold are strongly disrupted by major D_3 shear zones, and sulphide mineralization in these areas does not exhibit systematic variations. The most economically attractive orebodies in the deposit are distributed along the southern hinge of the fold, as a stacked series of three highly elongate ore shoots (e.g., the D lens and western portions of the J and JS lenses) that plunge steeply east and range up to 90 m in thickness (Figure 16). Despite the extraordinary thickness of sulphide, there is a lack of systematic variations in metal ratios, metal content and style of mineralization, and the shoots consist of relatively massive, copper-rich sulphide ore. In order to be practical for exploration purposes, any genetic model for the deposit must address the distribution, geometry, style and remarkable thickness of these orebodies, and provide an explanation for their spatial coincidence with the macroscopic F_2 hinge.

There are several possible models that may explain these features:

1) The fold-hinge orebodies were deposited in a fault-controlled basin as a stacked series of highly elongate sulphide lenses. During subsequent deformation, the thick, pyrite-rich (i.e., relatively competent) basin fill acted as a marked heterogeneity within the deforming rock mass that, as a consequence of strain perturbation, controlled the location and development of the macroscopic F_2 fold in the MSU. In this model, a syngenetic growth fault would roughly correspond to the short F_2 fold limb (Figure 24).
2) The fold-hinge orebodies were deposited in one or several fault-controlled basins, which were tectonically assembled into a D_1 thrust stack prior to F_2 folding. In this model, thrust stacking is favoured over structural repetition via isoclinal F_1 folding on the basis of the consistent facing directions of the J and JS lenses on the south limb of the macroscopic F_2 fold. The thick, fault-controlled orebodies could have formed within a single basin that was subsequently segmented by D_1 thrust faults, or within multiple basins that were juxtaposed during D_1 thrust faulting. The tectonically stacked basins controlled the location of the F_2 fold via the same mechanism outlined above.
3) The fold-hinge orebodies formed during internal remobilization of sulphide to accommodate hinge thickening and limb attenuation during isoclinal F_2 folding of three

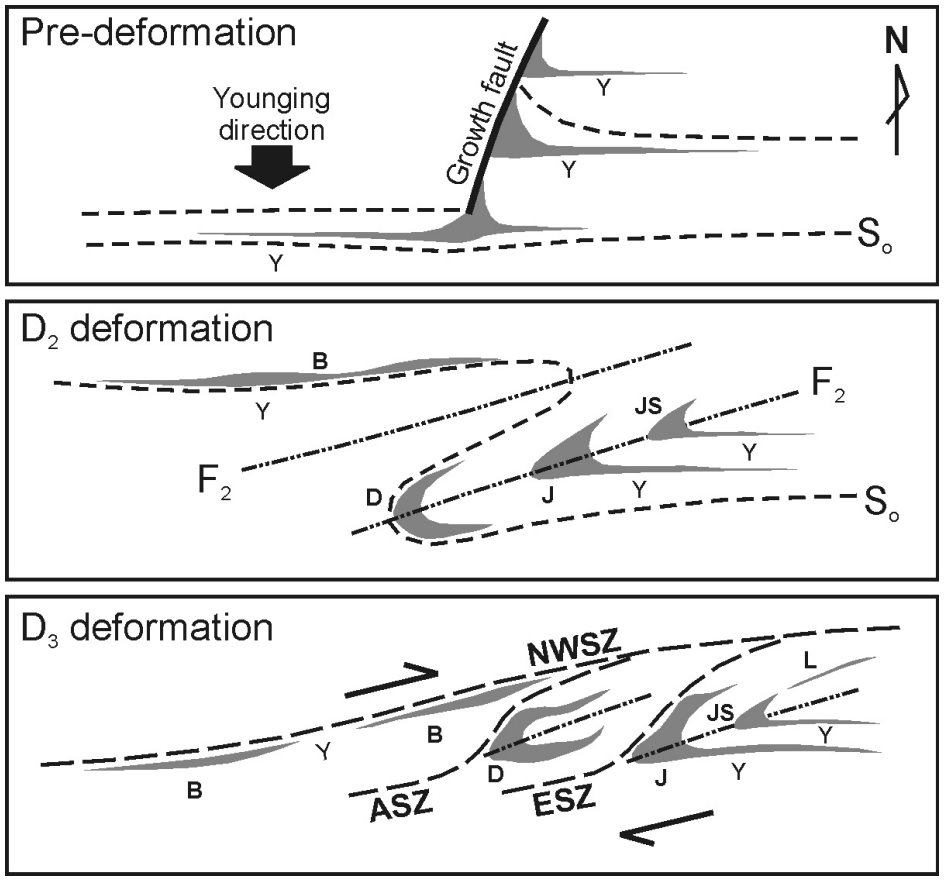

Figure 24: *Simplified cross-sections illustrating a possible genetic model for the major fold-hinge orebodies in the Ruttan deposit, which incorporates a synvolcanic growth fault that was subsequently transposed during D_2 isoclinal folding and D_3 shearing. See text for discussion.*

precursor sulphide layers. In this model, the primary zoning patterns in the precursor sulphide layers would have been obliterated by internal remobilization of sulphide into the macroscopic F_2 fold hinge in response to extreme attenuation of the short limb of the Z-asymmetric fold. The precursor lenses were stacked prior to F_2 folding, via either depositional or tectonic processes.

4) The fold-hinge orebodies result from bulk internal and external remobilization of sulphide into the southern F_2 fold hinge as a consequence of the intense structural overprint of the short limb and northern hinge of the F_2 fold during D_3 shearing.

5) A combination of one or more of these processes.

The fault basin–strain perturbation models (options 1 and 2) appear to provide viable explanations for the overall characteristics of the copper-rich orebodies, and can also explain their spatial coincidence with the macroscopic F_2 hinge. Unfortunately, however, such models are impossible to further constrain within the existing, poorly understood stratigraphic framework for the deposit. Although it could be argued that the massive, block-in-matrix style and copper-rich tenor of these orebodies are indicative of a fault-proximal depositional environment, these aspects must be reconciled with the virtual absence of clear examples of vent-proximal, stringer-style copper mineralization in the Main mine.

The remobilization models (options 3 and 4) are supported by the widespread evidence of sulphide remobilization on mesoscopic to submacroscopic scales in the deposit, which clearly indicates a high degree and locally large extent of internal and external remobilization, via both fluid- and solid-state processes. Hinge thickening is a natural consequence of tight to isoclinal folding, particularly in a mixed-layer system characterized by large competency contrasts, and sulphide remobilization is the only realistic mechanism to accomplish this in the case of a rheologically weak sulphide layer in a silicate-rock sequence. As described by Marshall and Gilligan (1993), preferential remobilization of rheologically weak sulphide phases (e.g., chalcopyrite) into the hinges of tight to isoclinal folds can produce substantial lateral variations in metal ratios within a folded sulphide layer. Hence, internal remobilization to accommodate hinge thickening (option 3) could conceivably explain both the extreme thickness and the relatively copper-rich character of the major fold-hinge orebodies. More difficult to reconcile, however, is the absence in these orebodies of the systematic primary zoning patterns observed on the long limbs of the F_2 fold. Given that such patterns are typically well preserved in documented examples of isoclinally folded sulphide deposits (e.g., van Staal and Williams, 1984; Marshall and Gilligan, 1993), it is unclear whether disruption during hinge thickening and internal remobilization of sulphide is a viable explanation for the massive, block-in-matrix style of the major fold-hinge orebodies.

Bulk remobilization of sulphide (option 4) would be expected to produce bodies of relatively copper-rich, transported ore that are largely devoid of primary depositional features and preferentially occur in relatively low-strain domains such as fold hinges or boudin necks. Entrainment of wallrock inclusions during bulk remobilization and transport of sulphide could also explain the macroscopic, block-in-matrix style of mineralization that characterizes the major fold-hinge orebodies. Mesoscopic examples of transported sulphide are common in the deposit and include the high-grade orebody exposed in the 25B2 stope on level WM690mL (Figure 8) that discordantly cuts a 2–3 m thick granodiorite sill. Overprinting relationships indicate that remobilization continued into the later stages of D_3 deformation, coeval with high-T, low-P metamorphism in the aureole of the Brehaut Lake pluton. In this context, it could be argued that bulk remobilization of sulphide into the relatively low-strain, southern hinge of the macroscopic F_2 fold was facilitated by thermally enhanced sulphide mobility during successor-arc magmatism and development of the major D_3 shear zones.

Unfortunately, no preference can be assigned to any of the above models based on the existing data. From an exploration perspective, however, each model predicts a genetic association between the most economically attractive orebodies in the Ruttan deposit and the macroscopic F_2 fold, and therefore represents a potentially important empirical exploration criterion. In particular, the fault basin–strain perturbation models would imply that the locations of the major F_2 fold closures along strike northeast of the Ruttan deposit may be controlled by undiscovered sulphide lenses in the Mine Sequence unit (MSU). Conversely, the remobilization models would predict that the location of remobilized sulphide orebodies might instead be controlled by F_2 fold hinges. Regardless, the authors conclude that the macroscopic F_2 fold closures should be a critical consideration in formulating exploration strategies and assessing the residual VMS potential of the MSU along strike from the Ruttan deposit, as well as on a regional scale in the Ruttan Block.

Acknowledgments

This project was made possible through the cooperation and generous logistical support of Hudson Bay Mining and Smelting Co., Limited, and particularly Bob Cooper (Mine Manager, Ruttan Operation). The authors thank Reg Yaworski, Steve Forgeron and Steve Kirby of the Mine Geology department for freely sharing their knowledge of the deposit, and their ideas regarding its genesis and subsequent modification. Enthusiastic assistance in core logging was provided by Paul Kremer and Jennifer Greville. George Gale is acknowledged for lively debate and discussion in the field. Accommodations during the core-logging component of this study were generously provided by David Corrigan of the Geological Survey of Canada.

References

Ames, D.E. 1991: The Ruttan Cu-Zn deposit and depositional environment: an update; *in* Report of Activities 1991, Manitoba Energy and Mines, Minerals Division, p. 106–107.

Ames, D.E. 1996: Stratigraphic and tectonic setting of the Paleoproterozoic Ruttan Cu-Zn VHMS deposit, Rusty Lake belt, Trans-Hudson Orogen; *in* EXTECH I: A Multidisciplinary Approach to Massive Sulphide Research in the Rusty Lake–Snow Lake Greenstone Belts, Manitoba, G.F. Bonham-Carter, A.G. Galley and G.E.M. Hall (ed.), Geological Survey of Canada, Bulletin 426, p. 15–43.

Ames, D.E. and Scoates, J.S. 1992: Geology, preliminary map of the geological setting of the Ruttan Cu-Zn deposit, Rusty Lake belt, Manitoba; Geological Survey of Canada, Open File 2571, scale 1:5000, with marginal notes.

Ames, D.E., Scoates, J.S. and Franklin, J.M. 1990: Preliminary report on the geological setting of the Ruttan base metal deposit and associated hydrothermal alteration, Rusty Lake volcanic belt, Manitoba (NTS 64B/5); *in* Report of Activities 1990, Manitoba Energy and Mines, Minerals Division, p. 179–186.

Ames, D.E. and Taylor, C. 1996: Geology of the West Anomaly orebody, Ruttan volcanic-hosted massive sulphide deposit, Proterozoic Rusty Lake belt; *in* EXTECH I: A Multidisciplinary Approach to Massive Sulphide Research in the Rusty Lake–Snow Lake Greenstone Belts, Manitoba, G.F. Bonham-Carter, A.G. Galley and G.E.M. Hall (ed.), Geological Survey of Canada, Bulletin 426, p. 45–76.

Ames, D.E., Van Breemen, O. and Scoates, J.S. 2002: Evidence for recycled Mesoarchean crust in the Ruttan arc succession, Rusty Lake belt, Trans-Hudson Orogen, Manitoba: U-Pb isotopic data; Radiogenic Age and Isotopic Studies: Report 15, Geological Survey of Canada, Current Research 2002-F2, 7 p.

Baldwin, D.A. 1980: Ruttan Lake, Karsakuwigamak Lake, Eagle Lake project (parts of 64B/5, 6, 11, 12); *in* Report of Field Activities 1980, Manitoba Energy and Mines, Mineral Resources Division, p. 14–18.

Baldwin, D.A. 1988: Geology of the southern part of the Rusty Lake volcanic belt; Manitoba Energy and Mines, Geological Services, Geological Report GR86-1, 90 p. plus 1:50 000-scale map.

Baldwin, D.A., Syme, E.C., Zwanzig, H.V., Gordon, T.M., Hunt, P.A. and Stevens, R.P. 1987: U-Pb zircon ages from the Lynn Lake and Rusty Lake metavolcanic belts, Manitoba: two ages of Proterozoic magmatism; Canadian Journal of Earth Sciences, v. 24, p. 1055–1063.

Barrie, C.T. and Taylor, C.F. 2001: Geology, alteration mineralogy, geochemistry and volcanogenic massive-sulphide potential of the Ruttan mine area and the southern Rusty Lake volcanic belt (NTS 64B); Manitoba Industry, Trade and Mines, Manitoba Geological Survey, Open File Report OF2001-9, 25 p. plus CD-ROM.

Beaumont-Smith, C.J. and Böhm, C.O. 2002: Structural analysis and geochronological studies in the Lynn Lake greenstone belt and its gold-bearing shear zones (NTS 64C10, 11, 12, 14, 15 and 16), Manitoba; *in* Report of Activities 2002, Manitoba Industry, Trade and Mines, Manitoba Geological Survey, p. 159–170.

Beaumont-Smith, C.J. and Böhm, C.O. 2003: Tectonic evolution and gold metallogeny of the Lynn Lake greenstone belt, Manitoba (NTS 64C10, 11, 12, 14, 15 and 16); *in* Report of Activities 2003, Manitoba Industry, Economic Development and Mines, Manitoba Geological Survey, p. 39–49.

Bickford, M.E., Collerson, K.D., Lewry, J.F., Van Schmus, W.R. and Chiarenzelli, J.R. 1990: Proterozoic collisional tectonism in the Trans-Hudson Orogen, Saskatchewan; Geology, v. 18, p. 14–18.

Corrigan, D. and Rayner, N. 2002: Churchill River–Southern Indian Lake Targeted Geoscience Initiative (NTS 64B, 64C, 64G, 64H), Manitoba: update and new findings; *in* Report of Activities 2002, Manitoba Industry, Trade and Mines, Manitoba Geological Survey, p. 144–158.

Gale, G.H. 2003: Vectoring volcanogenic massive sulphide deposits using rare earth elements and other pathfinder elements at the Ruttan mine, Manitoba (NTS 64B5); *in* Report of Activities 2003, Manitoba Industry, Economic Development and Mines, Manitoba Geological Survey, p. 54–73.

Gale, G.H. and McClenaghan, S.H. 2002: Determining residual mineral potential using europium anomalies in the Ruttan and Lynn Lake areas, Manitoba; *in* Report of Activities 2002, Manitoba Industry, Trade and Mines, Manitoba Geological Survey, p. 205–208.

Gale, G.H., McClenaghan, S.H. and Yaworski, R. 2002: Geology and geochemistry of the Ruttan and Darrol Lake deposits (NTS 63B5), Manitoba; *in* Report of Activities 2002, Manitoba Industry, Trade and Mines, Manitoba Geological Survey, p. 198–204.

Gilbert, H.P., Syme, E.C. and Zwanzig, H.V. 1980: Geology of the metavolcanic and volcaniclastic metasedimentary rocks in the Lynn Lake area; Manitoba Energy and Mines, Mineral Resources Division, Geological Paper GP80-1, 118 p.

Gilligan, L.B. and Marshall, B. 1987: Textural evidence for remobilization in metamorphic environments; Ore Geology Reviews, v. 2, p. 205–229.

Goodfellow, W.D., Grapes, K., Cameron, B. and Franklin, J.M. 1993: Hydrothermal alteration associated with massive sulfide deposits, Middle Valley, northern Juan de Fuca ridge; Canadian Mineralogist, v. 31, p. 1025–1060.

Gordon, T.M., Hunt, P.A., Bailes, A.H. and Syme, E.C. 1990: U-Pb ages from the Flin Flon and Kisseynew belts, Manitoba: chronology of crust formation at an Early Proterozoic accretionary margin; *in* The Early Proterozoic Trans-Hudson Orogen of North America, J.F. Lewry and M.R. Stauffer (ed.), Geological Association of Canada, Special Paper 37, p. 177–199.

Heaman, L.M., Erdmer, E. and Owen, J.V. 2002: U-Pb geochronologic constraints on the crustal evolution of the Long Range Inlier, Newfoundland; Canadian Journal of Earth Sciences, v. 39, p. 845–865.

Jackson, M.R. 1979: Stratigraphy and geochemistry of the Rusty Lake greenstone belt adjacent to the Ruttan mine, Manitoba; M.Sc. thesis, University of Manitoba, Winnipeg, Manitoba, 125 p.

Lin, S., Jiang, D. and Williams, P.F. 1998: Transpression (or transtension) zones of triclinic symmetry: natural example and theoretical modeling; *in* Continental Transpressional and Transtensional Tectonics, R.E. Holdsworth, R.A. Strachan and J.F. Dewey (ed.), Geological Society (London), Special Publication 135, p. 41–57.

Lucas, S.B., Stern, R.A., Syme, E.C., Reilly, B.A. and Thomas, D.J. 1996: Intraoceanic tectonics and the development of continental crust: 1.92–1.84 Ga evolution of the Flin Flon Belt, Canada; Geological Society of America Bulletin, v. 108, p. 602–629.

Lustig, G.N. 1979: Geology of the Fox orebody, northern Manitoba; M.Sc. thesis, University of Manitoba, Winnipeg, Manitoba, 87 p.

Marshall, B. and Gilligan, L.B. 1989: Durchbewegung structure, piercement cusps, and piercement veins in massive sulfide deposits: formation and interpretation; Economic Geology, v. 84, p. 2311–2319.

Marshall, B. and Gilligan, L.B. 1993: Remobilization, syn-tectonic processes and massive sulphide deposits; Ore Geology Reviews, v. 8, p. 39–64.

Olson, P.E. 1987: The stratigraphy, structural geology and geochemistry of the Fox Lake massive sulfide deposit; M.Sc. thesis, University of Manitoba, Winnipeg, Manitoba, 220 p.

Park, A.F. 1996: Structural evolution of sulphide tectonites and their host rocks, Stratmat mine, New Brunswick; Canadian Journal of Earth Sciences, v. 33, p. 472–492.

Rayner, N. and Corrigan, D. 2004: Uranium-lead geochronological results from the Churchill River–Southern Indian Lake transect, northern Manitoba; Geological Survey of Canada, Current Research 2004-F1, 14 p.

Reid, R.R. 1995: Ruttan structure; Hudson Bay Mining and Smelting Co., Ltd., Ruttan Operation, unpublished company report, 15 p.

Ryan, J.J. and Williams, P.F. 1999: Structural evolution of the eastern Amisk collage, Trans-Hudson Orogen, Manitoba; Canadian Journal of Earth Sciences, v. 36, p. 251–273.

Schwartz, T.C. and Brown, P. 2000: The Ruttan Mine exploration compilation project: mine model update and proposed drill targets for 2001; Hudson Bay Mining and Smelting Co., Ltd., Ruttan Operation, unpublished company report, 14 p.

Speakman, D.S., Chornoby, P.J., Haystead, B.C.W. and Holmes, G.F. 1982: Geology of the Ruttan deposit, northern Manitoba; *in* Precambrian Sulphide Deposits, H.S. Robinson Memorial Volume, R.W. Hutchinson, C.D. Spence, and J.M. Franklin (ed.), Geological Association of Canada, Special Paper 25, p. 525–555.

Stacey, J.S. and Kramers, J.D. 1975: Approximation of terrestrial lead isotope evolution by a two-stage model; Earth and Planetary Science Letters, v. 26, p. 207–221.

Stern, R.A., Machado, N., Syme, E.C., Lucas, S.B. and David, J. 1999: Chronology of crustal growth and recycling in the Paleoproterozoic Amisk collage (Flin Flon Belt), Trans-Hudson Orogen, Canada; Canadian Journal of Earth Sciences, v. 36, p. 1807–1827.

Stern, R.A., Syme, E.C., Bailes, A.H. and Lucas, S.B. 1995: Paleoproterozoic (1.90–1.86 Ga) arc volcanism in the Flin Flon Belt, Trans-Hudson Orogen, Canada; Contributions to Mineralogy and Petrology, v. 199, p. 117–141.

van Staal, C.R. and Williams, P.F. 1984: Structure, origin, and concentration of the Brunswick 12 and 6 orebodies; Economic Geology, v. 79, p. 1669–1692.

Whalen, J.B., Syme, E.C. and Stern, R.A. 1999: Geochemical and Nd isotopic evolution of Paleoproterozoic arc-type granitoid magmatism in the Flin Flon Belt, Trans-Hudson Orogen, Canada; Canadian Journal of Earth Sciences, v. 36, p. 227–250.

White, D.J., Zwanzig, H.V. and Hajnal, Z. 2000: Crustal suture preserved in the Paleoproterozoic Trans-Hudson orogen, Canada; Geology, v. 28, p. 527–530.

Zwanzig, H.V., Syme, E.C. and Gilbert, H.P. 1999: Updated trace element geochemistry of ca. 1.9 Ga metavolcanic rocks on the Paleoproterozoic Lynn Lake Belt; Manitoba Industry, Trade and Mines, Geological Services, Open File OF99-13, 48 p. plus data diskette and 1:100 000-scale map.